onstrated that there was a modest but significant decrease in ATP or CrP in either skeletal muscle, liver, or myocardium in rodent model of sepsis [40,41]. Thus, previous experimental and clinical observations have not reached a clear conclusion, possibly because of their study protocols or materials.

In view of the potential role of NO in myocardial energy metabolism, we have recently demonstrated that IL-1β-induced NO production decreases aerobic energy production through the direct inhibition of the mitochondrial respiratory enzymes, accelerates anaerobic glycolysis, and results in a significant decline in myocardial ATP content in cultured neonatal rat cardiac myocytes. Furthermore, we have suggested that the NO-induced energy disturbance induces the elevation of maximum diastolic potential, reduction of peak calcium current (I_{Ca}), and resultant contractile dysfunction [19]. In the present study, in order to notice the time-dependent effect of NO on aerobic respiration, we followed the time course of energy state up to 48 h after LPS administration, and could demonstrate that the activities of mitochondrial NADH-CoQ reductase, succinate-CoQ reductase, and ATPase were significantly lowered, and that in addition to ATP/ADP, myocardial ATP and CrP contents were significantly decreased, consistent with our above in vitro data. Thus, the evidence of bioenergetic abnormalities strongly suggests impaired mitochondrial function in the LPS-treated hearts. Recently, Gellerich et al. have reported that activities of mitochondrial complexes I and II are significantly decreased in the hearts of *Escherichia coli*-induced septic baboons [42]. By means of the skinned fiber technique, they also have shown that mitochondrial state three respiration and the activity of complexes I and III are reduced in the LPS-treated rabbit hearts [43]. Crouser et al. have reported that impaired mitochondrial respiratory dysfunction is strongly associated with the extent of mitochondrial ultrastructural abnormalities in LPS-induced septic cats [44]. Our data are therefore are in general agreement with these previous data and are extending the possibility that NO inactivates mitochondrial energy producing apparatus in beating hearts. The significance of our study may be supported also by the significant positive correlation between LVDP and myocardial ATP content as well as the disruption of mitochondrial ultrastructure in the hearts-treated with LPS for 48 h. Moreover, the findings that aminoguanidine significantly improved the LPS-induced functional and morphological disturbances in the mitochondria strongly suggest the possibility that NO plays a crucial role in sustained contractile failure in the endotoxemia via mitochondrial injury.

In view of myocardial energy balance, since the total ATP content was decreased to 82% of control in the LPS-treated hearts, it may be difficult to clearly explain how such a modest ATP decline is attributable to the cessation of contractility. We speculate that NO may induce a contraction–energy state mismatch which is well recognized in acute ischemia [45]. If NO could reduce the turnover rate of ATP in a small subcompartmentation, it would explain that even a small change in total ATP can have a large effect on the significant loss of contractility. Furthermore, NO may inactivate phosphocreatine energy shuttle or myosin ATPase activity, in addition to mitochondrial enzymes. Indeed, we have confirmed a modest but significant decrease in the activity of cytosolic Cr kinase (data not shown). However, we cannot exclude the possibility that NO-induced direct inactivation of calcium-regulating membrane proteins may also contribute to contractile dysfunction. Moreover, marked hemodynamic changes, such as a fall in BP and an increase in heart rates, were also seen after LPS injection. These facts suggest that many humoral and hemodynamic factors, as well as vasoactive agents other than NO may be involved in the causation of cardiac dysfunction. In the present study, LPS injection was followed by a marked elevation in plasma TNF-α levels, which has also been reported to directly suppress cardiac contractility [46]. Although there are still some other possibilities that NO may directly attack the molecules which regulate the contractility, our data provide the important possibility that NO-induced energy depletion affect the myocardial function, in which precise mechanism between modest ATP depletion and contractile disturbance should be further investigated in the future. Recently, Brealey et al. have reported that NO-induced mitochondrial dysfunction is associated with multi-organ failure in septic patients, strongly consistent with our data [47] knowledge that these detrimental effects of NO on mitochondrial enzymes may prove useful in designing protective therapies for endotoxin-induced myocardial injury.

In conclusion, the present study shows that sustained excessive NO production by iNOS in septic shock causes the mitochondrial dysfunction, resulting in myocardial energy depletion. The fact that myocardial function was correlated with cGMP levels in the early stage and with ATP levels in the later stage of septic shock suggests that NO may act at least at two levels to inhibit myocardial contractility; a rapid cGMP-mediated effect and a more sluggish one on oxidative metabolism. Although further study is required to clarify how energy depletion contributes to cell dysfunction, the present study provides strong evidence that excessive amounts of NO produced during endotoxemia can have significant detrimental effects on cardiac energy balance and contractility.

References

[1] Cohen J, Glauser MP. Septic shock: treatment. Lancet 1991;338:736–9.
[2] Parrillo JE. Pathogenetic mechanisms of septic shock. New Eng J Med 1993;328:1471–7.
[3] Klabunde RE, Coston AF. Nitric oxide synthase inhibition does not prevent cardiac depression in endotoxic shock. Shock 1995;3:73–8.
[4] Moncada S, Palmer RMJ, Higgs EA. Nitric oxide: physiology, pathophysiology, and pharmacology. Pharmacol Rev 1991;43:109–42.
[5] Titheradge MA. Nitric oxide in septic shock. Biochim Biophys Acta 1999;1411:437–55.
[6] Brady AJB, Poole-Wilson PA, Harding SE, Warren JB. Nitric oxide production within cardiac myocytes reduces their contractility in endotoxemia. Am J Physiol 1992:263:H1963–H1966.

[7] Balligand JL, Kelly RA, Marsden PA, Smith TW, Michel T. Control of cardiac muscle cell function by an endogenous nitric oxide signalling system. Proc Natl Acad Sci USA 1993;90:347–51.
[8] Finkel MS, Oddis CV, Jacob TD, Watkins SC, Hattler BG, Simmons RL. Negative inotropic effects of cytokines on the heart mediated by nitric oxide. Science 1992;257:387–9.
[9] Lange LG, Schreiner GF. Immune mechanisms of cardiac disease. New Eng J Med 1994;330(16):1129–35.
[10] Levine B, Kalman J, Mayer L, Fillit HM, Packer M. Elevated levels of tumor necrosis factor in severe chronic heart failure. New Eng J Med 1990;323:236–41.
[11] Katz SD, Rao R, Berman JW, Schwarz M, Demopoulis L, Bijiou R, et al. Pathophysiological correlates of increased serum tumor necrosis factor in patients with congestive heart failure: relation to nitric oxide dependent vasodilatation in the forearm circulation. Circulation 1994;90:12–6.
[12] Ramaciotti C, Sharkey A, McClellan G, Winegrad S. Endothelial cells regulate cardiac contractility. Proc Natl Acad Sci USA 1992;89: 4033–6.
[13] Shah AM, Spurgeon HA, Sollott SJ, Talo A, Lakatta EG. 8-Bromo cGMP reduces the myofilament response to calcium in intact cardiac myocytes. Circ Res 1994;74:970–8.
[14] Brady AJ, Warren JB, Poole-Wilson PA, Williams TJ, Harding SE. Nitric oxide attenuates cardiac myocyte contraction. Am J Physiol 1993;265:H176–H182.
[15] Gilbert EM, Haupt MT, Mandanas RY, Huaringa AJ, Carlson RW. The effect of fluid loading, blood transfusion, and catecholamine infusion on oxygen delivery and consumption in patients with sepsis. Am Rev Respir Dis 1986;134:873–8.
[16] Rackow EC, Asitz ME, Weil MH. Cellular oxygen metabolism during sepsis and shock: the relationship of oxygen consumption to oxygen delivery. JAMA 1988;259:1989–93.
[17] Geng Y, Hansson GK, Holme E. Interferon-gamma and tumor necrosis factor synergize to induce nitric oxide production and inhibit mitochondrial respiration in vascular smooth muscle cells. Circ Res 1992;71:1268–76.
[18] Wang D, McMillin JB, Bick R, Buja LM. Response of the neonatal rat cardiomyocyte in culture to energy depletion: effects of cytokines, nitric oxide, and heat shock proteins. Lab Invest 1996;75:809–18.
[19] Tatsumi T, Matoba S, Kawahara A, Keira N, Shiraishi J, Akashi K, et al. Cytokine-induced nitric oxide production inhibits mitochondrial energy production and impairs contractile function in rat cardiac myocytes. J Am Coll Cardiol 2000;35:1338–46.
[20] Decking UKM, Flesche CW, Godecke A, Schrader J. Endotoxin-induced contractile dysfunction in guinea pig hearts is not mediated by nitric oxide. Am J Physiol 1995;268:H2460–H2465.
[21] Tatsumi T, Matoba S, Kobara M, Keira N, Kawahara A, Tsuruyama K, et al. Energy metabolism after ischemic preconditioning in streptozotocin-induced diabetic rat hearts. J Am Coll Cardiol 1998; 31:707–15.
[22] Green LC, Wagner DA, Glogowski J, Skipper PL, Wishnok JS, Tannenbaum SR. Analysis of nitrate, nitrite, and [^{15}N] nitrate in biological fluids. Anal Biochem 1982;126:131–8.
[23] Honma M, Satoh T, Takezawa J, Ui M. An ultra sensitive method for the simultaneous determination of cyclic AMP and cyclic GMP in small volume samples from blood and tissue. Biochem Med 1977;18: 257–73.
[24] Lowry OH, Rosebrough NJ, Farr AL, Randall RJ. Protein measurement with the folin phenol reagent. J Biol Chem 1951;193:265–75.
[25] Bleistein J, Zierz S. Partial deficiency of complexes I and IV of the mitochondrial respiratory chain in skeletal muscle of two patients with mitochondrial myopathy. J Neurol 1989;236:218–22.
[26] Hatefi Y, Rieske JS. Preparation and properties of DPNH-coenzyme Q reductase (complex I of the respiratory chain). Method Enzymol 1967;X:235–9.
[27] Ziegler D, Rieske JS. Preparation and properties of succinate dehydrogenase-coenzyme Q reductase (complex II). Method Enzymol 1967;X:231–5.
[28] Lowe PN. Methods for studying heart mitochondrial ATPase in native and purified form. Method Study Cardiac Membr 1984;I:111–31.
[29] Sheperd D, Garland PB. Citrate synthase from rat liver. Method Enzymol 1969;13:11–6.
[30] Nagasaki A, Gotoh T, Takeya M, Yu Y, Takiguchi M, Matsuzaki H, et al. Coinduction of nitric oxide synthase, argininosuccinate synthase, and argininosuccinate lyase in lipopolysaccharide-treated rats. J Biol Chem 1996;271:2658–62.
[31] Balligand JL, Ungureanu D, Kelly RA, Kobzik L, Pimental D, Michel T, et al. Abnormal contractile function due to induction of nitric oxide synthesis in rat cardiac myocytes follows exposure to activated macrophage-conditioned medium. J Clin Invest 1993;91: 2314–9.
[32] Tsujino M, Hirata Y, Imai T, Kanno K, Eguchi S, Ito H, et al. Induction of nitric oxide synthase gene by interleukin-1β in cultured rat cardiocytes. Circulation 1994;90:375–83.
[33] Kapadia S, Lee J, Torre-Amione G, Birdsall HH, Ma TS, Mann DL. Tumor necrosis factor-α gene and protein expression in adult feline myocardium after endotoxin administration. J Clin Invest 1995;96: 1042–52.
[34] Schulz R, Panas DL, Catena R, Moncada S, Olley PM, Lopaschuk GD. The role of nitric oxide in cardiac depression induced by interleukin-1β and tumor necrosis factor-α. Br J Pharmacol 1995;114: 27–34.
[35] Hock CE, Yin K, Yue G, Wong P-K. Effects of inhibition of nitric oxide synthase by aminoguanidine in acute endotoxemia. Am J Physiol 1997;272:H843–H850.
[36] Meng X, Ao L, Brown JM, Fullerton DA, Banerjee A, Harken AH. Nitric oxide synthase is not involved in cardiac contractile dysfunction in a rat model of endotoxemia without shock. Shock 1997;7: 111–8.
[37] Hotchkiss RS, Karl IE. Reevaluation of the role of cellular hypoxia and bioenergetic failure in sepsis. JAMA 1992;267:1503–10.
[38] Hotchkiss RS, Song S-K, Neil JJ, Chen RD, Manchester JK, Karl IE, et al. Sepsis does not impair tricarboxylic acid cycle in the heart. Am J Physiol 1991;260:C50–C57.
[39] Solomon MA, Correa R, Alexander HR, Koev LA, Cobb JP, Kim DK, et al. Myocardial energy metabolism and morphology in a canine model of sepsis. Am J Physiol 1994;266:H757–H768.
[40] Brealey D, Karyampudi S, Jacques TS, Novelli M, Stidwill R, Taylor V, et al. Mitochondrial dysfunction in a long-term rodent model of sepsis and organ failure. Am J Physiol 2004:286:R491–R497.
[41] Watts JA, Kline JA, Thornton LR, Grattan RM, Brar SS. Metabolic dysfunction and depletion of mitochondria in hearts of septic rats. J Mol Cell Cardiol 2004;36:141–50.
[42] Gellerich FN, Trumbeckaite S, Hertel K, Zierz S, Muller-Werdan U, Werdan K, et al. Impaired energy metabolism in hearts of septic baboons: diminished activities of complex I and complex II of the mitochondrial respiratory chain. Shock 1999;11:336–41.
[43] Trumbeckaite S, Opalka JR, Neuhof C, Zierz S, Gellerich FN. Different sensitivity of rabbit heart and skeletal muscle to endotoxin-induced impairment of mitochondrial function. Eur J Biochem 2001; 268:1422–9.
[44] Crouser ED, Julian MW, Blaho DV, Pfeiffer DR. Endotoxin-induced mitochondrial damage correlates with impaired respiratory activity. Crit Care Med 2002;30:276–84.
[45] Gudbjarnason S, Mathes P, Ravens KG. Functional compartmentation of ATP and creatine phosphate in heart muscle. J Moll Cell Cardiol 1970;1:325–39.
[46] Bozkurt B, Kribbs SB, Clubb FJJ, Michael LH, Didenko VV, Hornsby PJ, et al. Pathophysiologically relevant concentrations of tumor necrosis factor-alpha promote progressive left ventricular dysfunction and remodeling in rats. Circulation 1998;97:1382–91.
[47] Brealey D, Brand M, Hargreaves I, Heales S, Land J, Smolenski R, et al. Association between mitochondrial dysfunction and severity and outcome of septic shock. Lancet 2002;360:219–23.

Aldosterone Directly Induces Myocyte Apoptosis Through Calcineurin-Dependent Pathways

Akiko Mano, MD; Tetsuya Tatsumi, MD, PhD; Jun Shiraishi, MD, PhD; Natsuya Keira, MD, PhD; Tetsuya Nomura, MD; Mitsuo Takeda, MD; Susumu Nishikawa, MD; Satoshi Yamanaka, MD, PhD; Satoaki Matoba, MD, PhD; Miyuki Kobara, MD, PhD; Hideo Tanaka, MD, PhD; Takeshi Shirayama, MD, PhD; Tetsuo Takamatsu, MD, PhD; Yoshihisa Nozawa, PhD; Hiroaki Matsubara, MD, PhD

Background—Aldosterone has recently attracted considerable attention for its involvement in the pathophysiology of heart failure, in which apoptotic cell loss plays a critical role. This study examined whether aldosterone directly induces myocyte apoptosis via its specific receptors.

Methods and Results—Neonatal rat cardiac myocytes were exposed to aldosterone (10^{-8} to 10^{-5} mol/L). Nuclear staining with Hoechst 33258 showed that aldosterone induced myocyte apoptosis in a dose- and time-dependent fashion. Treatment of myocytes with 10^{-5} mol/L aldosterone significantly increased the percentage of apoptosis ($15.5\pm1.4\%$) compared with serum-deprived control ($7.3\pm0.6\%$). Radio ligand binding assay revealed the existence of plasma membrane receptor with high affinity (K_d, 0.2 nmol/L) for aldosterone in cardiac myocytes but not in fibroblasts. Aldosterone rapidly ($\approx$30 seconds) mobilized $[Ca^{2+}]_i$ that was blocked by neomycin. Aldosterone induced dephosphorylation of the proapoptotic protein Bad, enhancement of mitochondrial permeability transition, decrease in mitochondrial membrane potential, and release of cytochrome c from the mitochondria into the cytosol with concomitant activation of caspase-3. These effects of aldosterone were inhibited by concurrent treatment with either an L-type Ca^{2+} channel antagonist, nifedipine, or inhibitors for the Ca^{2+}-dependent phosphatase calcineurin, cyclosporin A and FK506.

Conclusions—The present study demonstrates for the first time that the specific plasma membrane receptor (coupled with phospholipase C) for aldosterone is present on cardiac myocytes and that aldosterone accelerates the mitochondrial apoptotic pathway through activation of calcineurin and dephosphorylation of Bad, suggesting that the proapoptotic action of aldosterone may directly contribute to the progression of heart failure. **(*Circulation*. 2004;110:317-323.)**

Key Words: angiotensin ■ apoptosis ■ heart failure

Heart failure is a common, lethal condition associated with various cardiovascular diseases and remains a major cause of morbidity and mortality worldwide.[1] Cardiac myocytes are known to undergo apoptosis in some pathological conditions, such as hypoxia and ischemia-reperfusion.[2,3] Moreover, recent studies provide direct evidence that the progressive loss of cardiac myocytes by apoptosis is one of the most important components in the pathogenesis of heart failure.[4]

Several lines of evidence suggest that neurohormonal mechanisms play a central role in the progression of heart failure.[5] In addition to activation of the sympathetic nervous system, the renin-angiotensin-aldosterone system is known to have a deleterious effect on the heart. Recent studies report that aldosterone is produced in failing human hearts[6] and that aldosterone receptor antagonists, such as spironolactone and eplerenone, dramatically reduce morbidity and mortality from heart failure.[7,8] Aldosterone-mediated nongenomic action, such as rapid activation of protein kinase C and rise in $[Ca^{2+}]_i$ associated with phosphoinositide hydrolysis, is demonstrated in vascular smooth muscle cells (VSMCs) and endothelial cells.[9,10] However, it remains to be determined whether a specific plasma membrane receptor is present on cardiac myocytes.

Aldosterone-mediated action may cause various intracellular responses associated with elevation of $[Ca^{2+}]_i$. Recent studies have suggested that elevation of $[Ca^{2+}]_i$ induces apoptosis in some types of cells by activation of calcineurin, a Ca^{2+}-dependent phosphatase.[11] Because calcineurin affects the function of the proapoptotic protein Bad, which accelerates the mitochondrial death signaling pathway,[11] we hypothesized that aldosterone can directly induce myocyte apoptosis by activation of calcineurin.

This study was designed to determine whether cardiac myocytes have a plasma membrane receptor specific for aldosterone and whether aldosterone-mediated nongenomic

Received January 21, 2004; revision received April 1, 2004; accepted April 5, 2004.

From the Departments of Cardiovascular Medicine and Pathology and Cell Regulation (H.T., T.T.), Kyoto Prefectural University School of Medicine, Kyoto, and Pharmacobioregulation Research Laboratory (Y.N.), Taiho Pharmaceutical Co. Ltd, Iinou, Japan.

Correspondence to Tetsuya Tatsumi, MD, PhD, Department of Cardiovascular Medicine, Kyoto Prefectural University School of Medicine, Kawaramachi-Hirokoji, Kamigyo-ku, Kyoto 602-8566, Japan. E-mail tatsumi@koto.kpu-m.ac.jp

Circulation is available at http://www.circulationaha.org

DOI: 10.1161/01.CIR.0000135599.33787.CA

signaling affects myocyte apoptosis. We found that aldosterone directly induces myocyte apoptosis by activating its membrane receptor-mediated mitochondrial death signaling associated with the calcineurin-Bad pathway.

Methods

Cultured Neonatal Rat Cardiac Myocytes

Primary cultures of neonatal rat cardiac myocytes were prepared from neonatal Wistar rat hearts by digestion with 0.2% collagenase as described previously.[12] All experiments were performed 36 to 48 hours after incubation with DMEM containing 0.5% FBS.

Experimental Protocols

Myocytes were incubated with aldosterone (10^{-8} to 10^{-5} mol/L) for 24 hours or incubated with 10^{-5} mol/L aldosterone for the indicated periods (12 to 48 hours). To evaluate the effects of Ca^{2+} and calcineurin, myocytes were stimulated by 10^{-5} mol/L aldosterone for 24 hours after pretreatment with nifedipine (10^{-6} mol/L), calcineurin inhibitors, cyclosporin A (10^{-6} mol/L), and FK506 (10 μg/mL) for 1 hour. To examine Bad dephosphorylation, myocytes were incubated with 10^{-5} mol/L aldosterone for 4 hours. Control myocytes were incubated in serum-free DMEM.

Histochemical Determination of Apoptosis

Histochemical staining of myocytes was performed.[2] The cells were visualized by fluorescein microscopy, and the images were generated by dual-exposure photography. Apoptotic cells were identified on the basis of distinctive condensed or fragmented nuclear morphology, and apoptotic cell counts were expressed as a percentage of the total number of nuclei counted.[12]

Radioligand Binding Assay

Membrane fraction of myocytes and fibroblasts were prepared as previously described.[12,13] The fraction (50 μg of protein) was incubated for 1 hour at 37°C in a assay buffer. [1,2-^{3}H] aldosterone (Amersham, UK), specific activity of 39.8 Ci/mmol, was added at concentrations from 0.01 to 10 nmol/L. Incubates were transferred to Whatman GF/C filters (Whatman), and radioactivity was measured in a liquid scintillation counter. Specific binding was determined experimentally from the difference between counts in the absence and presence of 10 μmol/L cold unlabeled aldosterone. The *K*d and Bmax values were estimated by Scatchard analysis of the saturation data.

Intracellular Ca^{2+} Levels

Determination of $[Ca^{2+}]_i$ was performed as previously described.[10] Myocytes grown on glass base dishes were loaded with 2×10^{-6} mol/L fura-2 AM (Molecular Probes) for 1 hour at 37°C. Then myocytes were incubated with PBS and $[Ca^{2+}]_i$ images were visualized using Ion Optix dual-wavelength imaging system. Integration time was 0.017 seconds at each wavelength (340 and 380 nm), with a time increment of 0.1 seconds. The autofluorescence level was subtracted from each reading before calculation of $[Ca^{2+}]_i$. The system was calibrated by the method of Grynkiewicz et al.[14]

Mitochondrial Permeability Transition and Transmembrane Potential

Myocytes were loaded with 5×10^{-6} mol/L calcein-acetoxymethylester (calcein-AM, Molecular Probes) in the presence of 2 to 5×10^{-3} mol/L cobalt chloride to quench the cytoplasmic signals.[15] Then fluorescent intensities of the myocytes were determined. Loss of $\Delta\psi_m$ was assessed by Dye JC-1.[16] Cells grown on coverslips were incubated in PBS containing 10^{-5} mol/L JC-1 at 37°C for 5 minutes. Fluorescence emission at 527 and 590 nm was determined after excitation at 480 nm.

Immunoblotting

Antibodies for cytochrome c (7H8.2C12, PharMingen), Bad (Transduction Laboratories), phospho-Bad (Cell Signaling), and horseradish peroxidase–conjugated anti-IgG (Amersham) were used, and immunoblotting was performed as described.[12,13,17] Chemoluminescence was detected with ECL Western blot detection kits (Amersham).

Caspase-3 Activity

Caspase-3 enzymatic activity was determined with a CPP32 assay kit (MBL), which detects the production of the chromophore p-nitroanilide after its cleavage from the peptide substrate DEVD-p-nitroanilide, as described previously.[18]

Statistical Analysis

Data are expressed as mean±SE of at least 6 samples derived from more than 6 separate experiments. Skewed data (see Figure 3) were expressed as median (interquartile range). Differences were analyzed by 1-way ANOVA combined with the Bonferroni test. $P<0.05$ was considered to indicate statistical significance.

Results

Induction of Myocyte Apoptosis

Histochemical nuclear staining with Hoechst 33258 and immunohistochemical staining of cellular desmin showed that aldosterone increased apoptotic myocytes in a dose-dependent fashion (Figure 1A). Treatment of myocytes with 10^{-6} mol/L and 10^{-5} mol/L aldosterone significantly increased the percentage of myocyte apoptosis to 12.3% and 15.5%, respectively, compared with serum-deprived control (7.3%) (Figure 1B). Aldosterone 10^{-5} mol/L also increased apoptotic myocytes in a time-dependent fashion (Figures 1A and 1C). We also assessed the percentage of myocyte apoptosis by fluorescence-activated cell sorter analysis and ascertained that the percentage of apoptosis was almost compatible with that estimated by Hoechst 33258 staining (data not shown).[13] Treatment of myocytes with 10^{-5} mol/L aldosterone for 48 hours did not increase necrotic cell death as estimated by calcein acetoxymethyl ester and ethidium homodimer-1 staining or creatine kinase activity in the medium (data not shown).

Aldosterone Receptor on Plasma Membrane of Cardiac Myocytes

Specific saturable binding of aldosterone to plasma membranes of myocytes is illustrated in Figure 2. Scatchard analysis of specific binding in plasma membrane fraction shows maximum binding of 10.3±0.4 fmol/mg protein, with a calculated *K*d of 0.23±0.03 nmol/L. In contrast, no specific binding sites for aldosterone were detected in plasma membrane fraction from cardiac fibroblasts.

Intracellular Ca^{2+} Mobilization

Figure 3 illustrates the rapid induction of $[Ca^{2+}]_i$ by aldosterone in myocytes. Myocytes treated with aldosterone under Ca^{2+}-free conditions showed a rapid increase in fluorescence intensity reflecting the mobilization of $[Ca^{2+}]_i$ (Figure 3A). This phenomenon began within 30 seconds after addition and then slowly reached a plateau after 60 seconds. The median increase of $[Ca^{2+}]_i$ induced by aldosterone was 147 nmol/L (67 to 282 nmol/L) (Figure 3B). Neomycin, an inhibitor of

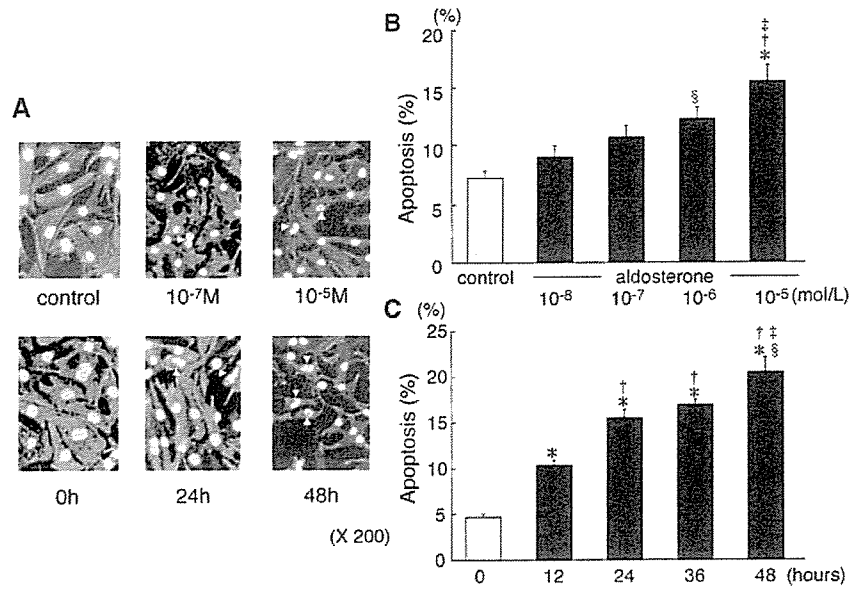

Figure 1. Aldosterone-induced myocyte apoptosis. A, Myocytes were treated with the indicated concentration of aldosterone for the indicated time periods. The myocytes were then stained with an anti-desmin polyclonal antibody and Hoechst 33258 (magnification ×200). Arrows indicate the typical feature of apoptotic myocytes. B, Dose dependency of aldosterone-induced myocyte apoptosis. Myocytes were treated with the indicated concentration of aldosterone (10^{-8} to 10^{-5} mol/L) for 24 hours. The percentage of apoptotic cells was calculated as described in Methods (n=6). *P<0.0001, §P<0.001 vs control; †P<0.0001 vs 10^{-8} mol/L; ‡P<0.01 vs 10^{-7} mol/L. C, Time course of aldosterone-induced myocyte apoptosis. Myocytes were treated with 10^{-5} mol/L aldosterone for the indicated time periods. The percentage of apoptotic cells was calculated as described in Methods (n=6). *P<0.0001 vs 0 hours; †P<0.0001 vs 12 hours; §P<0.001 vs 24 hours; ‡P<0.01 vs 36 hours.

phospholipase C, completely blocked this rapid effect of aldosterone (Figure 3C).

Effects of Ca^{2+} Antagonist and Calcineurin Inhibitors

Treatment of myocytes with aldosterone markedly increased apoptosis (2.2-fold), as estimated on the basis of nuclear morphology (Figure 4). When myocytes were pretreated with nifedipine, cyclosporin A, or FK506, the percentage of apoptotic myocytes was significantly (P<0.0001) decreased. Treatment of myocytes with nifedipine, cyclosporin A, or FK506 alone did not affect the percentage of apoptosis (data not shown). Cell length determined directly from the images using an edge-detection system[19] was decreased (43% to 48%, P<0.001, n=6) by addition of nifedipine (10^{-8} to 10^{-6} mol/L) but not cyclosporin A (10^{-6} mol/L) or FK506 (10 μg/mL), suggesting that contractile inhibition by Ca^{2+} channel antagonist or addition of calcineurin inhibitors is not involved in the cell survival.

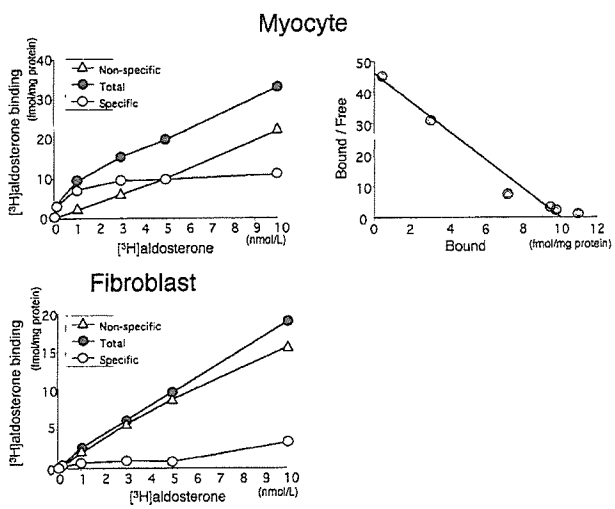

Figure 2. Binding of [^{3}H] aldosterone to cardiac myocytes and fibroblasts. Total, specific, and nonspecific binding of [^{3}H] aldosterone (0.01 to 10 nmol/L) to the membrane fractions of the myocytes (top left) and fibroblasts (bottom left) was examined. Representative tracings are shown from 4 independent experiments. ●, total binding; ○, specific binding; △, nonspecific binding. Scatchard analysis of the specific binding is performed in myocytes (top right).

Dephosphorylation of Bad

In the serum-deprived control, Bad consistently existed in highly phosphorylated form in the myocytes, whereas aldosterone markedly inhibited the Bad phosphorylation levels to 31% of the control and increased the dephosphorylation levels of Bad to 198% (Figure 5). This effect was maximum at 4 hours and then gradually decreased (data not shown). When myocytes were pretreated with nifedipine, cyclosporin A, or FK 506, dephosphorylation levels of Bad were substantially inhibited toward the control level.

Mitochondrial Permeability Transition, Membrane Potential, and Cytochrome C Release

Myocytes displayed punctate green-staining mitochondria, indicative of an intact mitochondrial membrane under control conditions. When myocytes were treated with aldosterone for 24 hours, green fluorescence in mitochondria was markedly reduced, consistent with permeability transition (PT) pore opening (Figure 6A, top). Pretreatment of myocytes with nifedipine, cyclosporin A, or FK506 significantly inhibited the loss of green fluorescence in mitochondria and thus prevented aldosterone-induced PT pore opening.

Myocytes showed red-orange mitochondrial staining by JC-1, indicative of normal high membrane potentials under control conditions.[20] In contrast, myocytes treated with aldosterone showed green fluorescence, indicating loss of $\Delta\psi_m$ (Figure 6A, bottom). Myocytes pretreated with nifedipine, cyclosporin A, or FK506 showed increased red-fluorescent intensity, indicating that $\Delta\psi_m$ was markedly preserved.

As shown in Figure 6, cytochrome c was detected only in the mitochondrial fraction under control conditions. Aldosterone inhibited the immunoreactivity of cytochrome c in

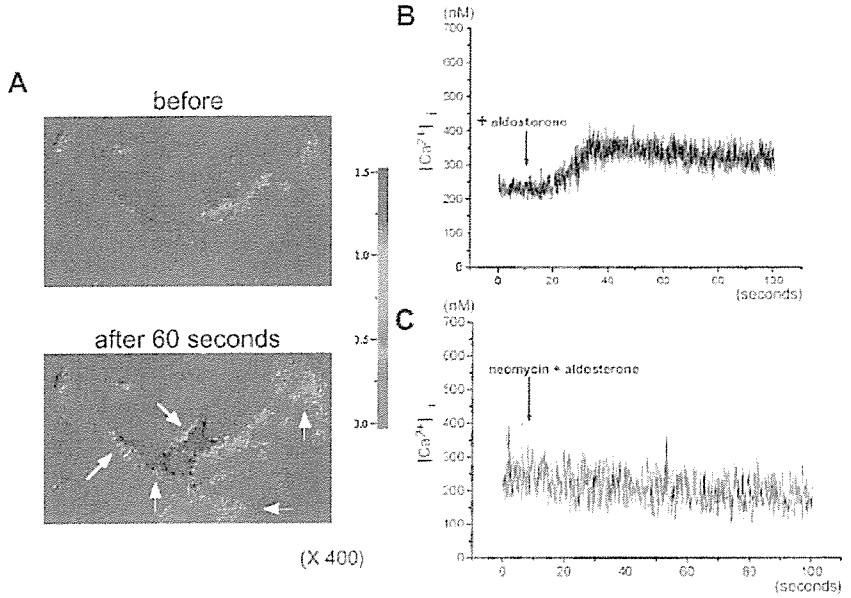

Figure 3. Calcium images and time course changes of $[Ca^{2+}]_i$ in myocytes. Myocytes were loaded with 2×10^{-6} mol/L fura-2 AM for 1 hour, and $[Ca^{2+}]_i$ was measured by dual-wavelength fluorescence of fura-2 in a microscopic cell-imaging system. A, Representative images (magnification ×400) of the myocytes are shown before and 60 seconds after addition of aldosterone (10^{-5} mol/L). Arrows show the myocytes with increased fluorescence intensity. B, Time course changes of $[Ca^{2+}]_i$ in the myocytes were measured before and after addition of aldosterone (10^{-5} mol/L). C, After pretreatment with neomycin (3×10^{-4} mol/L) for 15 minutes, myocytes were stimulated by aldosterone (10^{-5} mol/L), and $[Ca^{2+}]_i$ was determined. Tracings shown are representative from 5 independent experiments.

mitochondria to 36% of the control, whereas the activity in the cytosolic fraction was increased up to 395% of the control, which was inhibited by pretreatment with nifedipine, cyclosporin A, or FK506.

Activation of Caspase-3

Caspase-3 activity in the myocytes treated with aldosterone for 24 hours significantly increased by 1.4-fold compared with the serum-deprived control (Figure 7). Pretreatment with nifedipine, cyclosporin A, or FK506 inhibited the aldosterone-induced activation of caspase-3 to 1.1-fold, 1.1-fold, and 1.0-fold, respectively.

Discussion

The present study demonstrates for the first time that (1) aldosterone directly induces myocyte apoptosis in a dose- and time-dependent fashion; (2) plasma membrane receptor with high-affinity binding sites for aldosterone exists on cardiac myocytes but not cardiac fibroblasts; (3) aldosterone rapidly increases $[Ca^{2+}]_i$ associated with phospholipase C hydrolysis and induces dephosphorylation of Bad with enhancement of mitochondrial PT, decrease in $\Delta\psi_m$, release of cytochrome c from the mitochondria into the cytosol, and activation of caspase-3; and (4) aldosterone-mediated effects are inhibited by nifedipine, cyclosporin A, or FK506. Thus, our data clearly demonstrate that aldosterone induces a nongenomic intracellular response through phosphoinositide hydrolysis, resulting in stimulation of mitochondrial apoptotic pathway associated with calcineurin signaling and dephosphorylation of Bad.

In addition to the classic adrenal biosynthetic pathway, previous clinical and experimental studies have demonstrated the production of aldosterone and the presence of mineralocorticoid receptor in cardiovascular tissue.[21–23] Recent studies provide evidence that aldosterone rapidly increases $[Ca^{2+}]_i$ in endothelial cells and VSMCs by prompting transport of Ca^{2+}

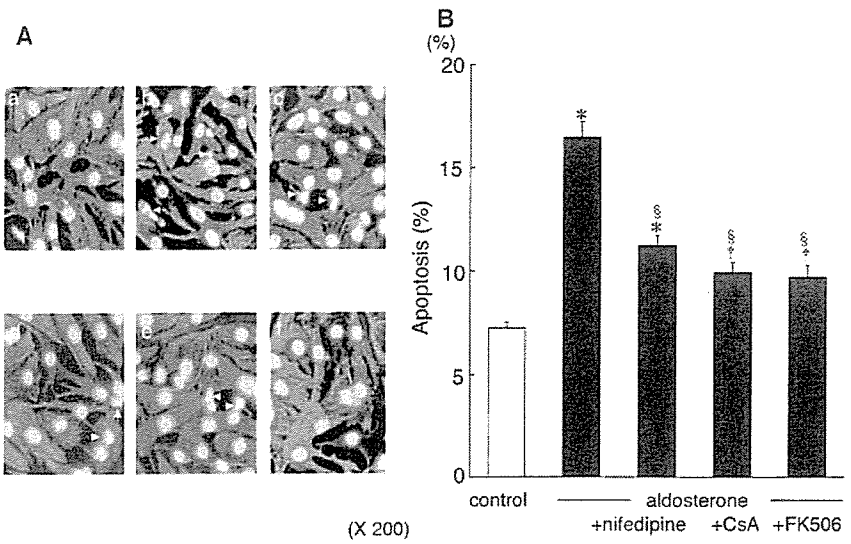

Figure 4. Histochemical characterization of apoptotic myocytes. After pretreatment with nifedipine (10^{-6} mol/L), cyclosporin A (CsA) (10^{-6} mol/L), or FK506 (10 μg/mL) for 1 hour, myocytes were stimulated by aldosterone (10^{-5} mol/L) for 24 hours. Myocytes were stained with an anti-desmin polyclonal antibody and Hoechst 33258. A, Representative micrographs (magnification ×200). a, control; b, aldosterone; c, aldosterone+nifedipine; d, aldosterone+CsA; e, aldosterone+FK506; f, CsA alone. B, Percentage of apoptotic myocytes. Myocyte apoptosis was calculated as described in Methods (n=6). *$P<0.0001$, †$P<0.001$ vs control; §$P<0.0001$ vs aldosterone.

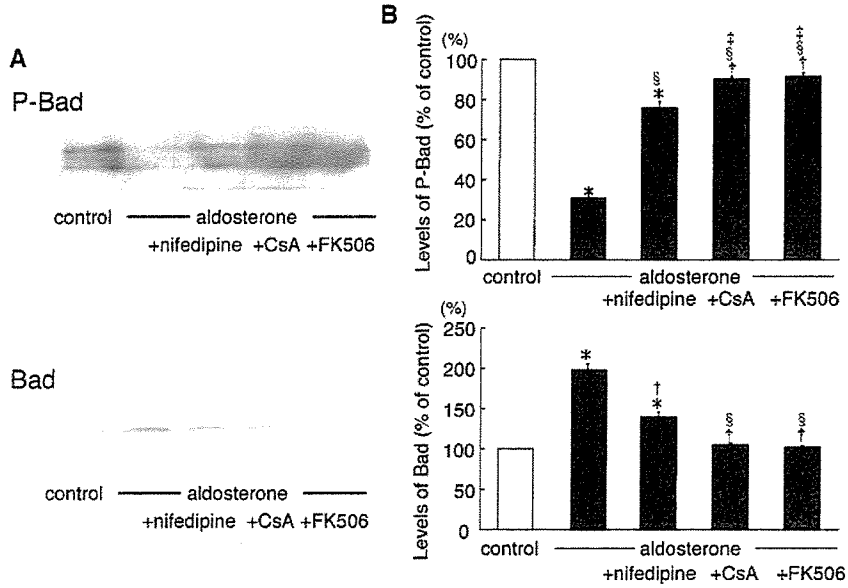

Figure 5. Western blot analysis of Bad. After pretreatment with nifedipine (10^{-6} mol/L), CsA (10^{-6} mol/L), or FK506 (10 μg/mL) for 1 hour, myocytes were stimulated by aldosterone (10^{-5} mol/L) for 4 hours. Cell extracts (55 μg protein) were probed with anti-phospho(P)-Bad or anti-Bad antibodies. A, Immunoblots shown are representative from 3 independent experiments. B, Densitometric analysis for dephosphorylation of Bad. Levels of P-Bad (top) and Bad (bottom) are shown as a percentage of change in the mean value derived from 3 independent experiments. Top, *P<0.0001, †P<0.01 vs control; §P<0.0001 vs aldosterone; ‡P<0.0001 vs aldosterone+nifedipine. Bottom, *P<0.0001 vs control; †P<0.0001 vs aldosterone; §P<0.001 vs aldosterone+nifedipine.

from storage sites via activation of phospholipase C, followed by an increase in inositol-1,4,5-triphosphate.[9,10] Such aldosterone-mediated nongenomic action was not observed in isolated adult rat cardiac myocytes; Benitah and Vassort[24] reported that Ca^{2+} current was increased by long-term incubation but not during short-term incubation (up to 6 hours) of aldosterone. This discrepancy between cardiac myocytes and VSMCs suggested that nongenomic aldosterone effects are restricted to specific target tissues. The present study showed for the first time the existence of the plasma membrane receptor specific for aldosterone in cardiac myocytes but not in cardiac fibroblasts, the binding affinity of which was very similar to that already reported in membrane fractions from human mononuclear leukocytes and pig kidneys (Kd, 0.23 nmol/L vs 0.1 to 0.4 nmol/L, respectively).[9] Furthermore, we found that nuclear fractions from myocytes have specific binding sites for aldosterone, with maximum binding of 504 fmol/mg protein and Kd of 1.2 nmol/L, suggesting that myocardial plasma membrane receptor is apparently different from intracellular receptor. Taken together, these data clearly indicate that cardiac myocytes and VSMCs possess a similar membrane receptor for aldosterone that is coupled with phospholipase C and that its activation leads to a rapid intracellular signaling cascade associated with $[Ca^{2+}]_i$ and protein kinase C.

Apoptosis is governed by families of proteins with positive and negative regulatory members acting at serial steps along a programmed pathway.[25] Bad is usually maintained in phosphorylated and sequestered form in the cytosol by 14-3-3 proteins and cannot exert its death-promotive action. However, when Bad is dephosphorylated by apoptotic signals, it heterodimerizes with Bcl-2 and Bcl-xL and suppresses their survival signals.[26] Recently, Ca^{2+}-mobilizing agents have been reported to dephosphorylate Bad by activating calcineurin and to augment Bad heterodimerization with Bcl-xL, leading to apoptosis.[11] In the present study, we have clearly shown that aldosterone decreases the phosphorylation levels of Bad and that this effect was significantly inhibited when myocytes were pretreated with an L-type Ca^{2+} channel antagonist or calcineurin inhibitors. Our findings therefore strongly suggest that Ca^{2+}-dependent calcineurin activation and dephosphorylation of Bad have a central role in the aldosterone-induced death-signaling pathway.

Mitochondria possesses the porin channel, called voltage-dependent-anion channel, in the outer membrane.[27] Binding of Bcl-xL protein to this channel usually closes (stabilizes) the PT pore. However, when Bad migrates into mitochondria and heterodimerizes with Bcl-xL, voltage-dependent-anion channel is opened. Thus, Bad increases mitochondrial PT and releases cytochrome c into the cytosol, with concomitant loss of $\Delta\psi_m$.[11,27] In our study, aldosterone induced PT pore opening, loss of $\Delta\psi_m$, release of cytochrome c into the cytosol, and activation of caspase-3, which were inhibited by concurrent treatment with nifedipine, cyclosporin A, or FK506. These findings indicate that aldosterone accelerates the mitochondrial apoptotic pathway triggered by calcineurin-induced dephosphorylation of Bad.

The level of aldosterone in plasma is approximately 10^{-7} mol/L in patients with heart failure, and the level of aldosterone in myocardium is approximately 17 times higher than that in plasma.[28,29] The aldosterone concentrations used in our study are therefore considered clinically relevant. Campbell et al[30] reported in aldosterone-treated rats that aldosterone caused myocyte necrosis by mitochondrial injury and sarcomeric contraction, because an increase in circulating aldosterone concentrations caused electrolyte imbalance, such as an enhanced potassium excretion, leading to activation of Na^+/H^+ and Na^+/Ca^{2+} exchange in cardiac mitochondria and sarcolemma. Taken together, in the in vivo situation in which the circulating aldosterone levels and electrolyte homeostasis are maintained, aldosterone may induce myocyte apoptosis rather than necrosis.

The present data indicate that nifedipine significantly inhibits the proapoptotic effect of aldosterone, suggesting that transsarcolemmal Ca^{2+} influx is also involved in aldosterone-induced increase in $[Ca^{2+}]_i$. Indeed, Benitah and Vassort[24]

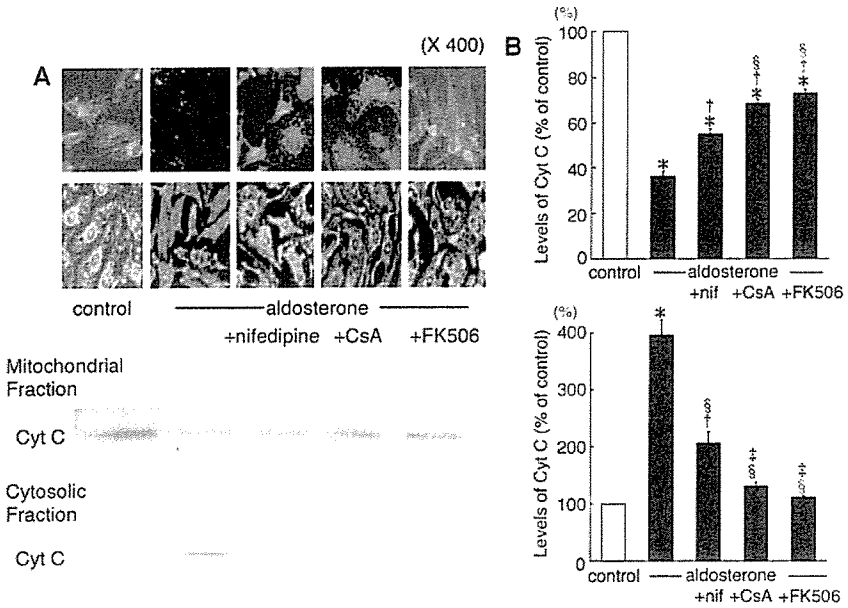

Figure 6. Changes of mitochondrial permeability transition, loss of mitochondrial transmembrane potential ($\Delta\psi_m$), and translocation of cytochrome c (Cyt C). A, Myocytes were stimulated by aldosterone (10^{-5} mol/L) for 24 hours after preincubation with nifedipine (10^{-6} mol/L), CsA (10^{-6} mol/L), or FK506 (10 μg/mL) for 1 hour. Mitochondrial PT and $\Delta\psi_m$ of the myocytes were monitored with calcein-AM and JC-1. Mitochondrial and cytosolic fractions (20 μg protein) were probed with antibody for Cyt C. Representative immunoblots are shown from 3 independent experiments. B, Densitometric analysis of Cyt C release. Levels of Cyt C are shown as a percentage of change in the mean values from 3 independent experiments compared with serum-deprived control. Top (mitochondrial fraction), *P<0.0001 vs control; †P<0.0001 vs aldosterone; §P<0.001 vs aldosterone+nifedipine (nif). Bottom (cytosolic fraction), *P<0.0001, †P<0.001 versus control; §P<0.0001 vs aldosterone; ‡P<0.01 vs aldosterone+nif.

have reported that aldosterone upregulates transsarcolemmal Ca^{2+} current into myocytes, probably by stimulating L-type Ca^{2+} channel subunit mRNA expression. Concurrent treatment of the myocytes with actinomycin D, an inhibitor of transcription, or cycloheximide, an inhibitor of protein synthesis, blunted the aldosterone-induced apoptosis (data not shown), therefore indicating that an L-type Ca^{2+} channel activation through a genomic effect is also partly involved in the effect of aldosterone. Thus, this evidence strongly supports the findings that calcineurin inhibitors were more effective than nifedipine in suppressing the proapoptotic effect of aldosterone.

In conclusion, our study has demonstrated that cardiac myocytes possess a plasma membrane receptor specific for aldosterone coupled with phospholipase C and that aldosterone induces myocyte apoptosis through a calcineurin-dependent mitochondrial death-signaling pathway triggered by rapid increase in intracellular Ca^{2+} levels. Aldosterone thus plays a crucial role in the progression of heart failure, and regulation of calcineurin and Bcl-2 family proteins may have important implications for the development of new therapeutic strategies for patients with heart failure.

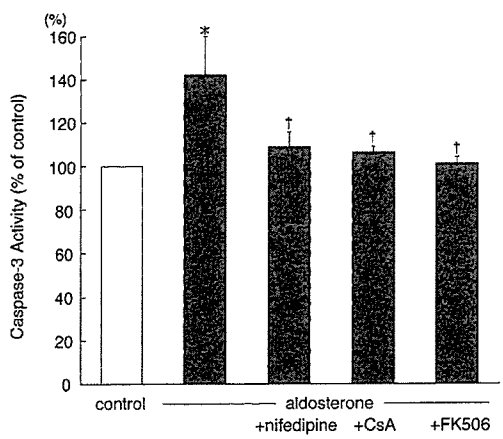

Figure 7. Caspase-3 activity in myocytes. Myocytes were subjected to pretreatment with nifedipine (10^{-6} mol/L), CsA (10^{-6} mol/L), or FK506 (10 μg/mL) for 1 hour, followed by aldosterone (10^{-5} mol/L) stimulation for 24 hours. Caspase-3 activity was determined as described in Methods. Activation level of caspase-3 is shown as a percentage of change in mean values of 6 samples derived from at least 3 separate experiments. *P<0.001 vs control, †P<0.01 vs aldosterone.

Acknowledgments

This study was supported in part by Grants-in-Aid from the Ministry of Education, Science and Culture and from the Ministry of Health Labor and Welfare, Japan.

References

1. Braunwald E, Bristow MR. Congestive heart failure: fifty years of progress. *Circulation.* 2000;102:IV14–IV23.
2. Tatsumi T, Shiraishi J, Keira N, et al. Intracellular ATP is required for mitochondrial apoptotic pathways in isolated hypoxic rat cardiac myocytes. *Cardiovasc Res.* 2003;59:428–440.
3. Fliss H, Gattinger D. Apoptosis in ischemic and reperfused rat myocardium. *Circ Res.* 1996;79:949–956.
4. Narula J, Haider N, Virmani R, et al. Apoptosis in myocytes in end-stage heart failure. *N Engl J Med.* 1996;335:1182–1189.
5. Packer M. The neurohormonal hypothesis: a theory to explain the mechanism of disease progression in heart failure. *J Am Coll Cardiol.* 1992;20:248–254.
6. Mizuno Y, Yoshimura M, Yasue H, et al. Aldosterone production is activated in the failing ventricles in human. *Circulation.* 2001;103:72–77.
7. Pitt B, Zannad F, Remme WJ, et al. The effect of spironolactone on morbidity and mortality in patients with severe heart failure: Randomized Aldactone Evaluation Study Investigators. *N Engl J Med.* 1999;341:709–717.
8. Pitt B, Remme W, Zannad F, et al. Eplerenone, a selective aldosterone blocker, in patients with left ventricular dysfunction after myocardial infarction. *N Engl J Med.* 2003;348:1309–1321.
9. Falkenstein E, Tillmann HC, Christ M, et al. Multiple actions of steroid hormones: a focus on rapid, nongenomic effects. *Pharmacol Rev.* 2000;52:513–556.
10. Wehling M, Neylon CB, Fullerton M, et al. Nongenomic effects of aldosterone on intracellular Ca^{2+} in vascular smooth muscle cells. *Circ Res.* 1995;76:973–979.
11. Wang HG, Pathan N, Ethell IM, et al. Ca^{2+}-induced apoptosis through calcineurin dephosphorylation of BAD. *Science.* 1999;284:339–343.

12. Shiraishi J, Tatsumi T, Keira N, et al. Important role of energy-dependent mitochondrial pathways in cultured rat cardiac myocyte apoptosis. *Am J Physiol Heart Circ Physiol.* 2001;281:H1637–H1647.
13. Yamanaka S, Tatsumi T, Shiraishi J, et al. Amlodipine inhibits doxorubicin-induced apoptosis in neonatal rat cardiac myocytes. *J Am Coll Cardiol.* 2003;41:870–878.
14. Grynkiewicz G, Poenie M, Tsien RY. A new generation of Ca^{2+} indicators with greatly improved fluorescence properties. *J Biol Chem.* 1985; 260:3440–3450.
15. Petronilli V, Miotto G, Canton M, et al. Imaging the mitochondrial permeability transition pore in intact cells. *Biofactors.* 1998;8:263–272.
16. Ankarcrona M, Dypbukt JM, Bonfoco E, et al. Glutamate-induced neuronal death: a succession of necrosis or apoptosis depending on mitochondrial function. *Neuron.* 1995;15:961–973.
17. Yang J, Liu X, Bhalla K, et al. Prevention of apoptosis by Bcl-2: release of cytochrome c from mitochondria blocked. *Science.* 1997;275: 1129–1132.
18. Casciola-Rosen L, Nicholson DW, Chong T, et al. Apopain/CPP32 cleaves proteins that are essential for cellular repair: a fundamental principle of apoptotic death. *J Exp Med.* 1996;183:1957–1964.
19. Tatsumi T, Matoba S, Kawahara A, et al. Cytokine-induced nitric oxide production inhibits mitochondrial energy production and impairs contractile function in rat cardiac myocytes. *J Am Coll Cardiol.* 2000;35: 1338–1346.
20. Cook SA, Sugden PH, Clerk A. Regulation of bcl-2 family proteins during development and in response to oxidative stress in cardiac myocytes: association with changes in mitochondrial membrane potential. *Circ Res.* 1999;85:940–949.
21. Slight SH, Joseph J, Ganjam VK, et al. Extra-adrenal mineralocorticoids and cardiovascular tissue. *J Mol Cell Cardiol.* 1999;31:1175–1184.
22. Harada E, Yoshimura M, Yasue H, et al. Aldosterone induces angiotensin-converting-enzyme gene expression in cultured neonatal rat cardiocytes. *Circulation.* 2001;104:137–139.
23. Lombes M, Oblin ME, Gasc JM, et al. Immunohistochemical and biochemical evidence for a cardiovascular mineralocorticoid receptor. *Circ Res.* 1992;71:503–510.
24. Benitah JP, Vassort G. Aldosterone upregulates Ca^{2+} current in adult rat cardiomyocytes. *Circ Res.* 1999;85:1139–1145.
25. Oltvani ZN, Korsmeyer SJ. Checkpoints of dueling dimers foli death wishes. *Cell.* 1994;79:189–192.
26. Zha J, Harada H, Yang E, et al. Serine phosphorylation of death agonist BAD in response to survival factor results in binding to 14–3–3 not Bcl-X(L). *Cell.* 1996;87:619–628.
27. Shimizu S, Narita M, Tsujimoto Y. Bcl-2 family proteins regulate the release of apoptogenic cytochrome c by the mitochondrial channel VDAC. *Nature.* 1999;399:483–487.
28. Rousseau MF, Gurne O, Duprez D, et al. Beneficial neurohormonal profile of spironolactone in severe congestive heart failure: results from the RALES neurohormonal substudy. *J Am Coll Cardiol.* 2002;40: 1596–1601.
29. Silvestre JS, Robert V, Heymes C, et al. Myocardial production of aldosterone and corticosterone in the rat: physiological regulation. *J Biol Chem.* 1998;273:4883–4891.
30. Campbell SE, Janicki JS, Matsubara BB, et al. Myocardial fibrosis in the rat with mineralocorticoid excess. *Am J Hypertens.* 1993;6:487–495.

Loss of Tie2 receptor compromises embryonic stem cell–derived endothelial but not hematopoietic cell survival

Isao Hamaguchi, Tohru Morisada, Masaki Azuma, Kyoko Murakami, Madoka Kuramitsu, Takuo Mizukami, Kazuyuki Ohbo, Kazunari Yamaguchi, Yuichi Oike, Daniel J. Dumont, and Toshio Suda

Tie2 is a receptor-type tyrosine kinase expressed on hematopoietic stem cells and endothelial cells. We used cultured embryonic stem (ES) cells to determine the function of Tie2 during early vascular development and hematopoiesis. Upon differentiation, the ES cell–derived Tie2$^+$Flk1$^+$ fraction was enriched for hematopoietic and endothelial progenitor cells. To investigate lymphatic differentiation, we used a monoclonal antibody against LYVE-1 and found that LYVE-1$^+$ cells derived from Tie2$^+$Flk1$^+$ cells possessed various characteristics of lymphatic endothelial cells. To determine whether Tie2 played a role in this process, we analyzed differentiation of *Tie2*$^{-/-}$ ES cells. Although the initial numbers of LYVE-1$^+$ and PECAM-1$^+$ cells derived from *Tie2*$^{-/-}$ cells did not vary significantly, the number of both decreased dramatically upon extended culturing. Such decreases were rescued by treatment with a caspase inhibitor, suggesting that reductions were due to apoptosis as a consequence of a lack of Tie2 signaling. Interestingly, *Tie2*$^{-/-}$ ES cells did not show measurable defects in development of the hematopoietic system, suggesting that Tie2 is not essential for hematopoietic cell development. (Blood. 2006;107:1207-1213)

Introduction

A close cell lineage relationship between hematopoietic and endothelial cells has long been recognized.[1,2] During embryogenesis, both cell types emerge in the yolk sac, and primitive erythrocytes differentiate juxtaposed to endothelial precursors by embryonic day 7.5 (E7.5).[3] In the mouse embryo, Tie2$^+$ cells in the aorta-gonad-mesonephros (AGM) region generate both blood and endothelial cells.[4] From studies of embryonic stem (ES) cell differentiation, vascular endothelial growth factor (VEGF)–responsive bipotent precursors of hematopoietic and endothelial cells, known as hemangioblasts, have been identified.[5] Hemangioblast-derived endothelial cells form vascular vessels through vasculogenesis and angiogenesis. Lymphatic development starts when a subset of vascular endothelial cells of the cardinal vein commit to a lymphatic lineage and sprout to form the primary lymph sacs at around E9 or 10.[6,7] Mouse molecular genetic experiments indicate that Prox-1 (a homeobox transcription factor) and the VEGF receptor 3 (VEGFR-3) are crucial for the commitment of endothelial cells to a lymphatic lineage.[8-10] Since lymphatic vessel–specific molecules are being identified, the molecular mechanisms underlying development of lymphatic cells as well as vascular and hematopoietic cells can now be analyzed.

Many studies report that expression of Flk1 is crucial for early establishment of endothelial and hematopoietic lineages and perhaps for their common progenitor.[5,11,12] Flk1 encodes a receptor tyrosine kinase for the vascular endothelial growth factor family of ligands.[13] Single Flk1$^+$ cells from embryoid bodies can give rise to blast colonies (blast lymphocyte colony-forming cells [BL-CFCs]), which produce both hematopoietic and endothelial cells in vitro.[5] Loss of Flk1 in mice results in selective defects in generating both blood and blood-vessel endothelial cells (BECs).[11] In addition to Flk1, Flt1 and Tie2 tyrosine kinases are also expressed in immature hematopoietic cells and BECs.[14-17]

The expression pattern of Tie2 suggests a function in both vascular endothelial and hematopoietic cells. Recently we determined the function of Ang1/Tie2 signaling, which maintains long-term repopulating hematopoietic stem cells in the bone marrow niche, suggesting that Tie2 signaling is crucial for adult bone marrow hematopoiesis.[18] In the mouse vitelline artery at E9.5, Tie2$^+$ hematopoietic cells aggregate and adhere to endothelial cells.[19] In vitro culture of Tie2$^+$ cells isolated from the AGM region generates both blood and endothelial cells.[4] In fetal liver, the Tie2$^+$ fraction contains an enriched fraction of long-term repopulating cells.[20] Based on these findings, Tie2 signaling was thought to regulate embryonic development and differentiation of hematopoietic cells. However, more recently, Puri and Berstein have demonstrated that Tie2 is dispensable for embryonic hematopoiesis using ES cell mouse chimeras.[21] This finding suggests that Tie2 function in developmental hematopoiesis differs from its role in bone marrow hematopoiesis.

From the Department of Cell Differentiation, The Sakaguchi Laboratory, School of Medicine, Keio University, Tokyo, Japan; Department of Safety Research on Blood and Biological Products, National Institute of Infectious Diseases, Tokyo, Japan; Department of Medical Biophysics, University of Toronto, ON, Canada; and the Division of Molecular and Cellular Biology Research, Sunnybrook and Women's Research Institute, Toronto, ON, Canada.

Submitted May 5, 2005; accepted September 27, 2005. Prepublished online as *Blood* First Edition Paper, October 11, 2005; DOI 10.1182/blood-2005-05-1823.

Supported in part by Grants-in-Aid from Ministry of Education, Science, Technology, Sports, and Culture, Japan; and by a research grant from the Human Frontiers Science Program Organization.

Reprints: Isao Hamaguchi, Department of Safety Research on Blood and Biological Products, National Institute of Infectious Diseases, 4-7-1 Gakuen, Musashimurayama, Tokyo 208-0011, Japan; e-mail: 130hama@nih.go.jp; or Toshio Suda, The Sakaguchi Laboratory of Developmental Biology School of Medicine, Keio University, Shinanomachi 35, Shinjuku, Tokyo 160-8582, Japan; e-mail: sudato@sc.itc.keio.ac.jp.

The publication costs of this article were defrayed in part by page charge payment. Therefore, and solely to indicate this fact, this article is hereby marked "advertisement" in accordance with 18 U.S.C. section 1734.

By contrast, Tie2 function in BECs has been intensively analyzed at both developmental and adult stages. In vivo and in vitro experiments show that Tie2 signaling potently induces sprouting, chemotaxis, and network formation.[22,23] Furthermore, the Tie2 ligand Ang1 is a potent survival factor for BECs under serum deprivation.[24] A role for Tie2 signaling in blood vessel endothelial survival in vivo has also been illustrated using conditional rescue of *Tie2*$^{-/-}$ embryos,[25] further supporting a role of this signaling system in endothelial cell survival.

Recently it has been demonstrated in mice that Tie2 is expressed and functions in lymphatic vessels embryonically[26] and in adults.[27] Tie2-deficient mice exhibit severe defects in vascular and heart development and die by E9.5,[28,29] making analysis of the lymphatic system difficult. Therefore, here we analyzed the function of Tie2 in lymphatic endothelial cells (LECs) and hematopoietic cells as well as in developing BECs using differentiation of cultured ES cells. We identify ES cell–derived LECs as well as BECs and hematopoietic cells, and demonstrate that Tie2 signaling is essential for development of BECs and LECs, but not for hematopoietic cells.

Materials and methods

Cell preparation and culture conditions

TT2,[30] E14,[31] and R1[32] ES cells were maintained on mouse embryonic fibroblast (MEF) feeder cell layers in knockout Dulbecco-modified Eagle medium (Gibco BRL, Carlsbad, CA) containing 15% fetal bovine serum (Intergen, Purchase, NY), 100 U/mL leukemia inhibitory factor (LIF; Chemicon International, Temecula, CA), 0.1 mM nonessential amino acids (Gibco BRL), 1 mM sodium pyruvate (Gibco BRL), 2 mM L-glutamine (Gibco BRL), and 100 μM 2-mercaptoethanol (Sigma-Aldrich, St Louis, MO). After removal of LIF, ES cells were cultured on collagen type IV plates (Becton Dickinson, San Jose, CA) at 1×10^4 cells/mL for 2 days. Cells were then disaggregated by trypsin and seeded on OP9 cells at 1×10^5 cells/mL. After 5 days of culture, OP9 cells were removed from ES cells through a Sephadex G10 column (Amersham Bioscience, Uppsala, Sweden), and the ES cells were fractionated by Flk1 and Tie2 expression using FACSvantage (Becton Dickinson). Sorted cells were seeded on OP9 cells at 1000 to 15 000 cells/mL and cultured in the presence of VEGF-C (100 ng/mL; R&D Systems, Minneapolis, MN), VEGF-D (100 ng/mL; R&D Systems), or the caspase inhibitor Z-VAD-fmk (10-100 nM; Calbiochem, La Jolla, CA). When indicated, sorted cells were cultured with recombinant soluble Tie2-Fc fusion protein (30 μg/mL)[19] or recombinant soluble CD4-Fc fusion protein (30 μg/mL).[19]

Immunocytochemistry

Immunocytochemistry was performed essentially as described.[33] Differentiated ES cells cultured on OP9 cells were fixed with 4% paraformaldehyde at 4°C and stained with a rat monoclonal anti-mouse platelet–endothelial cell adhesion molecule 1 (PECAM-1) monoclona antibody (mAb) (MEC13.3; Becton Dickinson) or a rat monoclonal anti-mouse LYVE-1 antibody (ALY7[26]) by the indirect immunoperoxidase method using horseradish peroxidase–conjugated anti-rat IgG. Peroxidase activity was visualized using 3,3′-diaminobenzidine (Dojindo, Kumamoto, Japan). To determine whether Prox-1 was expressed in LYVE-1$^+$ cells, we stained cells with biotinylated ALY7 and anti–Prox-1 antibody (Covance, Berkeley, CA). LYVE-1 and Prox-1 expression was detected by reacting with Alexa 488–conjugated Streptavidin (Molecular Probes, Eugene, OR) and Alexa 546–conjugated goat anti-rabbit antibody (Molecular Probes), respectively. For nuclear staining, cells were treated with TOTO3 (Molecular Probes). Stained cells were visualized by fluorescence microscopy. Stained and unstained cells were visualized by fluorescent microscopy (IX71) with either UplanApo 4×/0.13 NA, 10×/0.40 NA, or 20×/0.70 NA objectives (Olympus, Tokyo, Japan). Images were further processed with Adobe Photoshop (Adobe Systems, San Jose, CA). For DiI labeling, 10 μg/mL DiI-Ac-LDL (Molecular Probes) was added to differentiated ES cells on OP9 cells and adherent cells were incubated for 4 hours at 37°C. After removing the media containing DiI-Ac-LDL, cells were washed and stained with anti–PECAM-1 (FITC-conjugated; Becton Dickinson) or anti–LYVE-1 (biotin-conjugated) plus FITC-conjugated Streptavidin (Becton Dickinson). Uptake of DiI-Ac-LDL by blood vessel endothelial cells (PECAM-1$^+$ cells) and lymphatic endothelial cells (LYVE-1$^+$ cells) was visualized using a standard rhodamine excitation emission filter (Olympus, Tokyo, Japan).

RT-PCR analysis

Total RNA was extracted from cells using RNeasy Kit (Qiagen, Hilder, Germany). Isolated RNA was reverse-transcribed using an reverse transcriptase (RT) for polymerase chain reaction (PCR) Kit (Clontech, Palo Alto, CA). cDNAs were amplified using Taq polymerase (TaKaRa, Kyoto, Japan). Sequences of gene-specific primers for RT-PCR were as follows: *GATA2*, 5′-(acacaccacccgatacccacctat), 3′-(cctacgccatggcagtcaccatgct); *SCL*, 5′-(cgcggatccacggagcggccgccgagcgcg), 3′-(cggaattccgcgccgcactacttt-tggtgtg); c-myb, 5′-(gacagaagaggaggacagaatca), 3′-(tctcagggtcttcgtcgt-tatag); *AML1*, 5′-(ccagcaagctgaggagcggcg), 3′-(cggatttgtaaagacggtga); *Tie2*, 5′-(ttagttctctgtggagtcag), 3′-(aggccctgagttcttcactc); *Flk1*, 5′-(agaacac-caaaagagaggaacg), 3′-(gcacacaggcagaaaccagtag); *VEGFR3*, 5′-(gctaccact-gctactacaag), 3′-(gataatcccagtcgaaggtg); *Prox1*, 5′-(aagtggttcagcaatttccg), 3′-(tgaccttgtaaatggccttc); *LYVE1*, 5′-(ttcctcgcctctatttggac), 3′-(tctgttgtct-gcgtttcatcc); *Pdpn*, 5′-(gtgccagtgttgttctgggt), 3′-(tctgttgtctgcgtttcatcc); *Evi1*, 5′-(aatatgagtcatgccaaccc), 3′-(cttggtgtactgacatcatc); and *GAPDH*, 5′-(aatcccatcaccatcttcca), 3′-(ccaggggtcttactccttg).

PCR products were separated on a 1.2% agarose gel and gels were stained with ethidium bromide.

Quantitative RT-PCR analysis

Total RNA was isolated from 10^4 cells and cDNA was reverse-transcribed using Superscript III (Invitrogen, Carlsbad, CA) according to the manufacturer's instructions. The expression levels of Ang1, Ang2, and Ang3 were analyzed by quantitative (Q) RT-PCR using a LightCycler instrument (Roche Diagnostics, Mannheim, Germany) with LightCycler software version 3.5. cDNA was amplified for Q-PCR using SYBR Green I (Sigma-Aldrich) to detect PCR product. cDNA (2 μL) was used in a 20-μL final volume reaction containing 10 μL SYBR Premix Ex Taq (TaKaRa), 0.4 μM *Ang1* forward (5′-GCCTTTGCACTAAAGAAGGTGTTTT-3′), and 0.4 μM *Ang1* reverse (5′-ATACATCCGCACAGTCTCGAAATG-3′). The LightCycler was programmed to run an initial denaturation step at 95°C for 10 seconds followed by 45 cycles of denaturation (95°C for 5 seconds) and extension (60°C for 20 seconds), monitoring the synthesis of product at the end of the extension step of each cycle. The same conditions were used with primers *Ang2* forward (5′-AGGAGATCAAGGCCTACTGT-GACA-3′) and *Ang2* reverse (5′-GCTCCCGAA GCCCTCTTTG-3′), and *Ang3* forward (5′-GTTCCAGGACTGTGCAGAGATCA-3′) and *Ang3* reverse (5′-TCTCCATGTCACAGAACACCTTGAG-3′). The Ang1, Ang2, and Ang3 values were normalized against mouse β-actin (forward 5′-CAGCCTTCCTTCT-TGGGTATGG-3′; reverse 5′-CTGTGTTGGCATAGAGGTC TTTACG-3′).

Flow cytometric analysis and cell sorting

The following mAbs used for flow cytometry were purchased from Becton Dickinson: anti-CD34 (RAM34), anti–c-Kit (ACK45), anti–Sca-1 (E13-161.7), anti–CD45 (30-F11), anti–Flk1 (Avas12α1), anti–PECAM-1 (MEC13.3), anti–Mac-1 (M1/70), anti–Gr-1 (RB6-8C5), and anti–TER-119. Also used were anti-Tie2 mAb (TEK4)[34] and anti–LYVE-1 mAb (ALY7).[26] Fluorescence-activated cell sorting (FACS) analysis was performed on a FACSvantage (Becton Dickinson).

Progenitor assay by methylcellulose culture

Tie2$^+$Flk1$^+$ or Flk1$^+$ cells derived from ES cells were embedded in 1 mL alpha medium containing 1.3% methylcellulose (1500 cp; Sigma-Aldrich), 30% fetal calf serum (FCS), 1% deionized bovine serum albumin (BSA;

Sigma-Aldrich), 0.1 mM 2-mercapto-ethanol (Sigma-Aldrich), 10 ng/mL stem cell factor (SCF; PeproTech EC, London, United Kingdom), 10 ng/mL recombinant mouse interleukin-3 (IL-3; PeproTech EC), 10 ng/mL recombinant human IL-6 (PeproTech EC), and 2 U/mL recombinant human erythropoietin (Epo; Chugai Pharmaceutical, Tokyo, Japan). Cells were cultured in a 35-mm culture dish and incubated at 37°C in a humidified atmosphere with 5% CO_2.

Statistics

Data are expressed as means plus or minus standard deviation (SD). Statistical analysis was conducted using the Student *t* test. Statistical significance was defined as a *P* value less than .05.

Results

In vitro differentiation of ES cells

In order to analyze the function of Tie2 in the development of LECs as well as BECs and hematopoietic cells, we developed a cell culture system for ES cell differentiation. After removal of LIF, E14 ES cells were cultured on collagen type IV plates for 2 days to initiate differentiation to a mesoderm lineage; subsequently, cells were transferred to OP9 stromal cells. Markers of both endothelial and hematopoietic cells, Sca-1, c-kit, and CD34, were expressed in undifferentiated ES cells (Figure 1A). Although 1% of ES cells expressed Flk1 on collagen plates, Tie2 was not expressed in Flk1$^+$ cells (data not shown). Following transfer of cells on collagen plates to OP9 cells, 8% of Flk1$^+$ cells expressed Tie2 on day 3 of culture. Numbers of Tie2$^+$ cells increased until day 5 of culture, when Tie2 expression was maximal; thereafter, both expression levels and numbers of Tie2$^+$ cells gradually decreased. At day 9 of culture, cells cocultured with OP9 cells began expressing CD45, a marker of all hematopoietic cells except mature erythrocytes. Since Tie2$^+$ cells appeared just before CD45$^+$ hematopoietic cells, Tie2$^+$ cells in the Flk1$^+$ cell fraction may represent hematopoietic progenitor cells. We examined other ES strains, such as TT2 and R1 cells, using the same culture conditions, and confirmed that these strains showed a similar mesodermal phenotypes as E14 cells (data not shown).

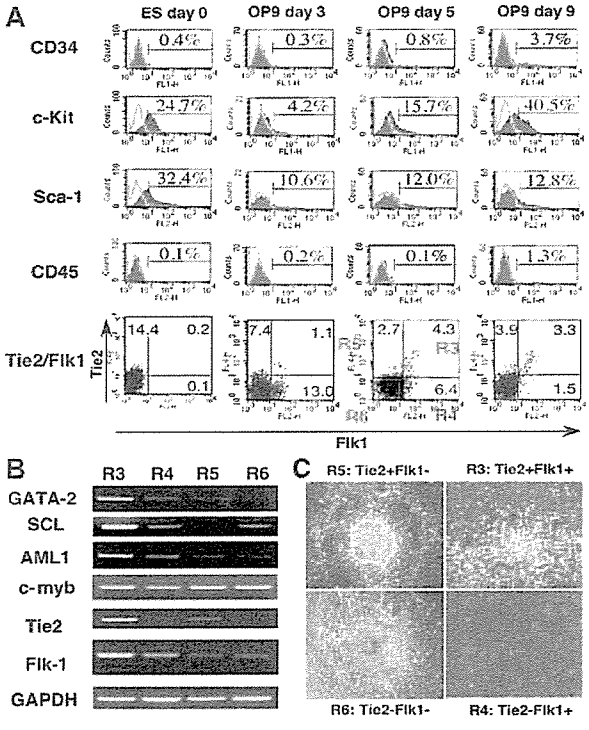

Figure 1. Mesodermal differentiation of ES cells on OP9 stromal cells. (A) E14 ES cells were cultured on collagen type IV plates for 2 days, and then all cells were cultured on OP9 cells for 9 days. The expression of CD34, c-Kit, Sca-1, CD45, Flk1, and Tie2 in ES cell–derived cells was analyzed at the indicated time points by flow cytometry. Stained *Tie*$^{-/-}$ cells are represented by purple shaded histograms. Unstained controls are represented by green lines. The percentages of cells in each quadrant are indicated. (B) Gene expression of fractionated cells shown in A (R3-R6) was analyzed by RT-PCR. (C) Fractionated cells (20 000; R3-R6) were cultured on OP9 cells. On day 7 of culture, hematopoietic clusters (red arrowheads) were developed only from the R3 fraction. In other fractions (R4-R6) hematopoietic clusters were not developed, but embryoid body–like colonies (blue arrowheads) developed from R5 and R6 fractions. Cells were analyzed at low (×40) magnification.

Development of hematopoietic, lymphatic endothelial, and blood vessel endothelial cells from Flk1$^+$Tie2$^+$ cells

To analyze the differentiating potential of ES-derived cells, we fractionated cells on day 5 of culture using Tie2 and Flk1 mAb as shown in Figure 1A (bottom panel, R1-R4). Expression profiling of transcription factors specific for hematopoietic or endothelial cells was undertaken by RT-PCR (Figure 1B). Expression levels of GATA-2, SCL, and AML-1 in the Tie2$^+$Flk1$^+$ fraction (R3) were 1.7-, 2.5-, and 1.7-fold higher than those in the Tie2$^-$Flk1$^+$ fraction (R4), respectively. In the Flk1$^-$ fraction (R5 and R6), expression levels of these genes were much lower compared with the Tie2$^-$Flk1$^+$ fraction (R4), suggesting that the Tie2$^+$Flk1$^+$ fraction may contain committed progenitors of hematopoietic and endothelial lineages. Cells (20 000) fractionated by Flk1 and Tie2 expression were cultured on OP9 cells (Figure 1C), and hematopoietic clusters formed only from the Tie2$^+$Flk1$^+$ fraction (R3) (Figure 1C, red arrowheads). Hematopoietic clusters were not detected in Flk1$^+$Tie2$^-$ (R4), Flk1$^-$Tie2$^+$ (R5), or Flk1$^-$Tie2$^-$ fractions (R6). The number of hematopoietic progenitors in each fraction was estimated by colony-forming assays in methylcellulose culture (Figure 2A-B). BECs were detected by staining with PECAM-1 mAb (Figure 2C). PECAM-1$^+$ endothelial cells were spindle shaped and took up an acetyl-LDL (Figure 2D). To detect LECs, we generated a mAb against LYVE-1 (ALY7), a receptor for extracellular matrix glycosaminoglycan. Using this mAb, we detected LYVE-1$^+$ cells on OP9 cells (Figure 2E). These cells also took up acetyl-LDL (Figure 2F), and 65% of them expressed Tie2 (Figure 2I). The lymphatic identity of these cells was further demonstrated by RT-PCR, using primers specific for LEC-enriched genes, namely, *Pdpn*, *VEGFR3*, and *Prox1* (Figure 2J). Furthermore, LYVE-1$^+$ cells coexpressed Prox-1 (Figure 2K). The presence of VEGFR-3 transcripts in these cultures provided the impetus for us to add the lymphatic growth factors, VEGF-C and VEGF-D. The addition of these factors resulted in a marked increase in the number of LYVE-1$^+$ cells (Figure 2L) and an increase in the size of monolayers (VEGF-C, Figure 2G; VEGF-D, Figure 2H). These findings suggest that LYVE-1$^+$ cells derived from ES cell differentiation cultures express many genes that are restricted to or enriched in LECs.

That Tie2 is required for these cell types is supported by the more than 10-fold increase in hematopoietic, blood vessel endothelial, and lymphatic endothelial colonies from Tie2$^+$Flk1$^+$ cells compared with Tie2$^-$Flk1$^+$ or Tie2$^-$Flk1$^-$ cell fractions (Table 1). To determine which cells produce the Tie2 ligands Ang1, Ang2, and Ang3 in order to support Tie2$^+$ cells, we performed quantitative expression analysis for Ang1, Ang2, and Ang3. As shown in Figure 2M, OP9 cells and LYVE-1$^-$ ES-derived cells expressed Ang1 but not Ang2 or Ang3. Although low expression levels of

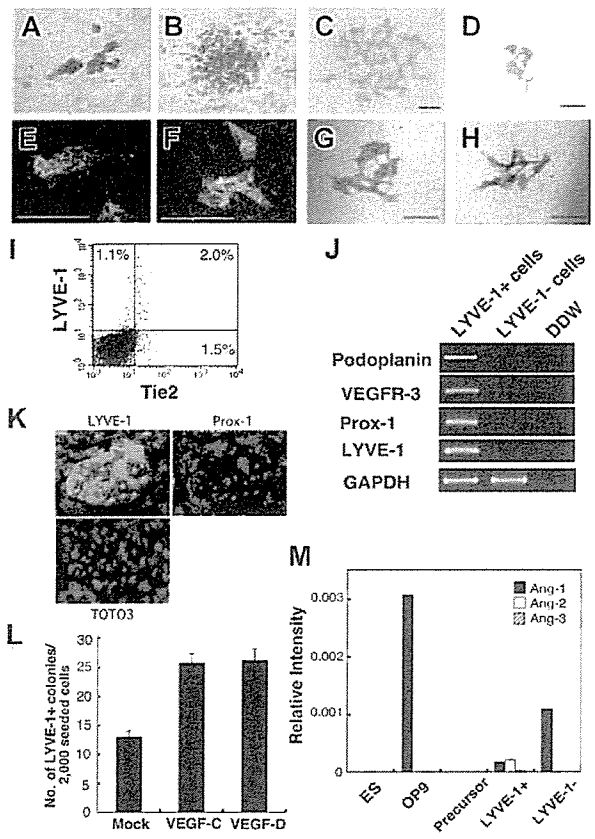

Figure 2. Development of lymphatic endothelial cells from ES cells. The Tie2$^-$Flk1$^+$ fraction of ES cell–derived cells formed erythroid colonies (A) and granulocyte-macrophage colonies (B) in methylcellulose. Vascular and lymphatic endothelial cells were stained with PECAM-1 mAb (C) and LYVE-1 mAb (D), respectively. PECAM-1$^+$ cells (green, panel E) and LYVE-1$^+$ cells (green, panel F) took up acetyl-LDL (red, panels E and F). Scale bars, 10 μm. (I) Expression of LYVE-1 and Tie2 in differentiated cells derived from ES cells on OP9 cells on day 6 of culture was analyzed by flow cytometry. The percentages of cells in each quadrant are indicated. (J) Lymphatic-specific genes, *Pdpn*, VEGFR-3, and Prox-1 in LYVE-1$^+$ and LYVE-1$^-$ cells were analyzed by RT-PCR. (K) Immunostaining at high magnification (× 200) showed that LYVE-1$^+$ cells (green) coexpressed Prox-1 (red). TOTO3 (blue) was used to stain nuclei. (L) In the presence of VEGF-C and VEGF-D (100 ng/mL each), the number of LYVE-1$^+$ colonies increased to 2 times that of mock-treated cells. Colonies were also larger in the presence of VEGF-C and VEGF-D (panels G and H, respectively). Results are expressed as the mean ± SD. (M) OP9 and ES cell–derived LYVE-1$^-$ cells expressed Ang1. LYVE-1$^+$ cells expressed low levels of Ang1 and Ang2. Ang1, Ang2, and Ang3 were not detectable in ES cells and lymphatic precursors (Flk1$^+$ cells derived from ES cells).

Ang1 and Ang2 were detected in LYVE-1$^+$ cells, ES cells and lymphatic precursor cells (ES cell–derived Flk1$^+$ cells) did not express Ang's. These results suggest that Ang1 derived from OP9 cells might affect the growth or survival of Tie2$^+$ cells.

Table 1. Frequency of hematopoietic and endothelial progenitors of differentiated ES cells

	Erythroid colonies from 30 000 cells	GM colonies from 30 000 cells	Vascular endothelial colonies from 1500 cells	Lymphatic endothelial colonies from 2000 cells
Tie2$^-$Flk1$^+$	11.3 ± 6.4	11.7 ± 2.1	47.5 ± 5.3	24.3 ± 2.5
Tie2$^-$Flk1$^+$	0	0	5.2 ± 1.8	0
Tie2$^+$ Flk1$^-$	0	0	0	0
Tie2$^-$Flk1$^-$	0	0	0	0
Bulk	0	0	2.7 ± 1.5	1.3 ± 0.6

Development of hematopoietic and endothelial cells from Tie2-deficient ES cells

To clarify the function of Tie2 during hematopoietic and endothelial differentiation from ES cells, the differentiation capacity of *Tie2*$^{-/-}$ ES cells was examined using our culture system. *Tie2*$^{-/-}$ ES cells grew normally on MEF feeder layer cells (data not shown), and differentiated cells grown on OP9 cells were analyzed by flow cytometry. The frequency of cells expressing Flk1 in the *Tie2*$^{-/-}$ ES cells was similar to that seen in *Tie2*$^{+/-}$ cells (Figure 3A). RT-PCR of RNA from this fraction for expression of the genes involved in development of hematopoietic and endothelial cells revealed no remarkable differences between *Tie2*$^{+/-}$ and *Tie2*$^{-/-}$ cells (Figure 3B). To analyze hematopoietic development of *Tie2*$^{-/-}$ ES cells, we calculated the number of hematopoietic clusters formed on OP9 cells at day 7 of culture. The number and size of hematopoietic clusters of *Tie2*$^{-/-}$ ES cells were the same as those of *Tie2*$^{+/-}$ cells (Figure 3C, and data not shown). When the *Tie2*$^{-/-}$ hematopoietic clusters were transferred to fresh OP9 cells for an additional week, normal proliferating hematopoietic cells were detected by flow cytometry. Mature Mac-1–, Gr-1–, and Ter119–positive hematopoietic cells were differentiated from *Tie2*$^{-/-}$ ES cells (Figure 3D), and the frequency of mature hematopoietic cells was similar to that seen in *Tie2*$^{+/-}$ cells (data not shown), suggesting that Tie2 is not essential for development of hematopoietic cells. By contrast, *Tie2*$^{-/-}$ ES cells were severely defective in forming blood vessel and lymphatic endothelial colonies on OP9 cells at day 6 of culture. The number of such blood vessel and lymphatic endothelial colonies was approximately one

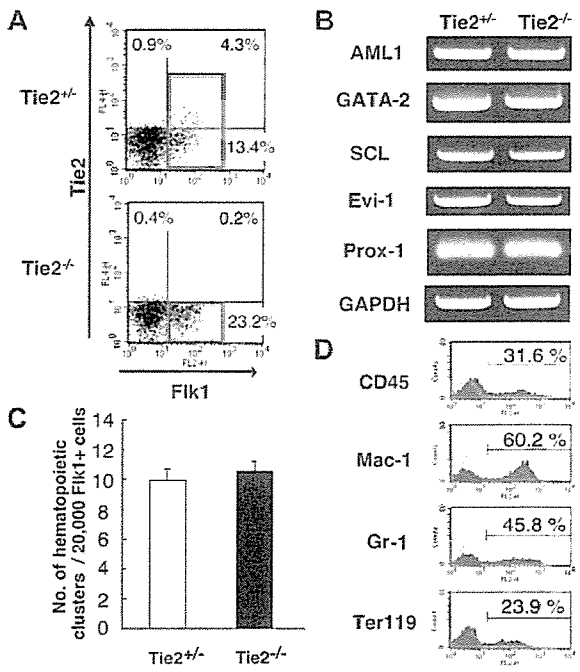

Figure 3. Normal development of hematopoietic cells from *Tie2*$^{-/-}$ ES cells. (A) FACS analysis of the expression of Flk1 and *Tie2* in *Tie2*$^{-/-}$ and *Tie2*$^{+/-}$ ES cell–differentiated cells. Red squares show the Flk1$^+$ fraction. The percentages of cells in each quadrant are indicated. (B) Expression of genes associated with mesoderm in Flk1$^+$ cells shown in panel A (red squares) was analyzed by RT-PCR. (C) Flk1$^+$ cells (20 000) were cultured on OP9 cells. The number of hematopoietic clusters from *Tie2*$^{-/-}$ and *Tie2*$^{-/-}$ cells at day 7 of culture was calculated. Results are expressed as the mean ± SD. (D) *Tie2*$^{-/-}$ hematopoietic clusters were cultured for an additional 7 days on fresh OP9 cells. The expression of CD45, Mac-1, Gr-1, and Ter119 was analyzed by flow cytometry. ES cell–derived hematopoietic cells are represented by purple shaded histograms; unstained controls, by green lines.

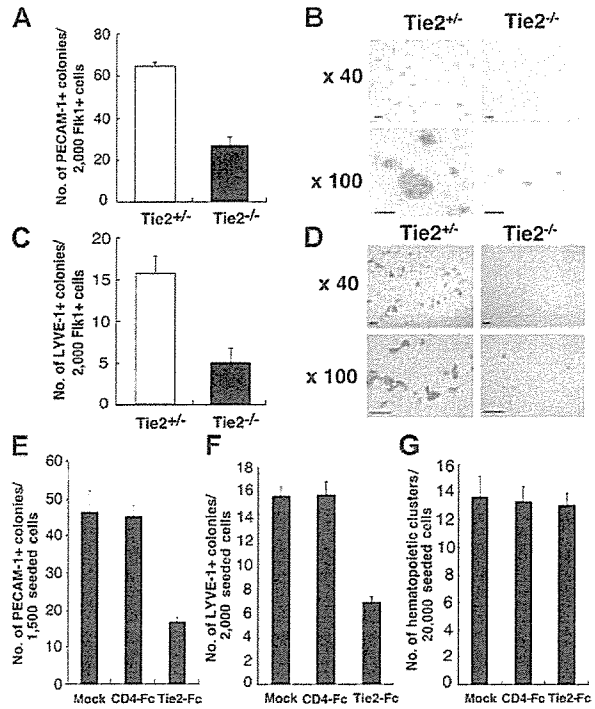

Figure 4. Lymphatic and blood vessel endothelial cell development from *Tie2*$^{-/-}$ ES cells. (A) Flk1 cells (2000) were cultured on OP9 cells. At day 7 of culture, the number of vascular endothelial colonies developed from *Tie2*$^{+/-}$ (□) and *Tie2*$^{-/-}$ (■) ES cells was calculated. (B) Vascular endothelial colonies were stained with PECAM-1 mAb and analyzed at low (× 40) and high (× 100) magnification. (C) The number of lymphatic endothelial colonies developed from *Tie2*$^{-/-}$ (□) and *Tie2*$^{-/-}$ (■) ES cells was calculated. (D) Lymphatic endothelial colonies were stained with LYVE-1 mAb and analyzed at low (× 40) and high (× 100) magnification. Scale bars in panels B and D, 20 μm. In the presence of Tie2-Fc (30 μg/mL), the number of vascular and lymphatic endothelial colonies was decreased (panels E and F, respectively). (G) Hematopoietic cluster formation was not affected by exogenous soluble Tie2-Fc (30 μg/mL). Exogenous soluble CD4-Fc (30 μg/mL) served as the control. Results in panels A, C, and E-G are expressed as the mean ± SD.

third that observed from *Tie2*$^{+/-}$ cells (Figure 4A-B), and colony size was smaller than that seen from *Tie2*$^{+/-}$ cells (Figure 4C-D). These results suggest that Tie2 function is required for development of BECs and LECs, but not of hematopoietic cells. To confirm these findings, we added soluble Tie2-Fc fusion protein to the culture media of wild-type ES cells to block Tie2 signaling. As shown in Figure 4E-G, the number of vascular and lymphatic endothelial cell colonies derived from wild-type ES cells in the presence of soluble Tie2-Fc fusion protein decreased to one half to one third of the mock-treated cells, while the number of hematopoietic clusters was not affected by soluble Tie2-Fc fusion protein. We did not detect such inhibition in the presence of soluble CD4-Fc fusion protein (Figure 4 E-F).

Tie2 signaling is crucial for antiapoptotic signaling in the development of lymphatic and blood vessel endothelial cells

To further analyze the mechanisms underlying defective proliferation of BECs and LECs from *Tie2*$^{-/-}$ ES cells, we analyzed expression of blood vessel– and lymphatic-specific markers PECAM-1 and LYVE-1, respectively, by flow cytometry at days 2, 4, and 6 of culture (Figure 5A). Cells expressing PECAM-1 and LYVE-1 in *Tie2*$^{-/-}$ ES cells decreased over 6 days. PECAM-1$^+$ cells in *Tie2*$^{-/-}$ cells were approximately one third the number of those in *Tie2*$^{+/-}$ cells at day 6 of culture, as was the case with LYVE-1$^+$ cells (Figure 5B-C). This finding suggested that *Tie2*$^{-/-}$-mediated signaling protects endothelial cells from cell death. To test this possibility, we treated *Tie2*$^{-/-}$ cells with the caspase inhibitor Z-VAD-fmk. As shown in Figure 5B and C, lymphatic and blood vessel endothelial colony formation was rescued in the presence of Z-VAD-fmk in a dose-dependent fashion. In the presence of 50 nM of Z-VAD-fmk, the number of lymphatic endothelial colonies from *Tie2*$^{-/-}$ cells was rescued to 60% of that from *Tie2*$^{+/-}$ cells (Figure 5C), although the size of *Tie2*$^{-/-}$ lymphatic endothelial colonies remained small (Figure 5D). The formation of blood vessel endothelial colonies was similar in the presence of Z-VAD-fmk (50 nM; Figure 5C). These findings suggest that Tie2 signaling is crucial for LEC and BEC development and mediates antiapoptotic signaling during ES cell differentiation.

Discussion

Although we have demonstrated that Tie2 is expressed in the vitelline artery,[19] the AGM region,[4] and fetal liver,[20] the function of Tie2 in development has not been elucidated. The early death of Tie2$^{-/-}$ embryos precludes detailed analysis of the role of Tie2 in

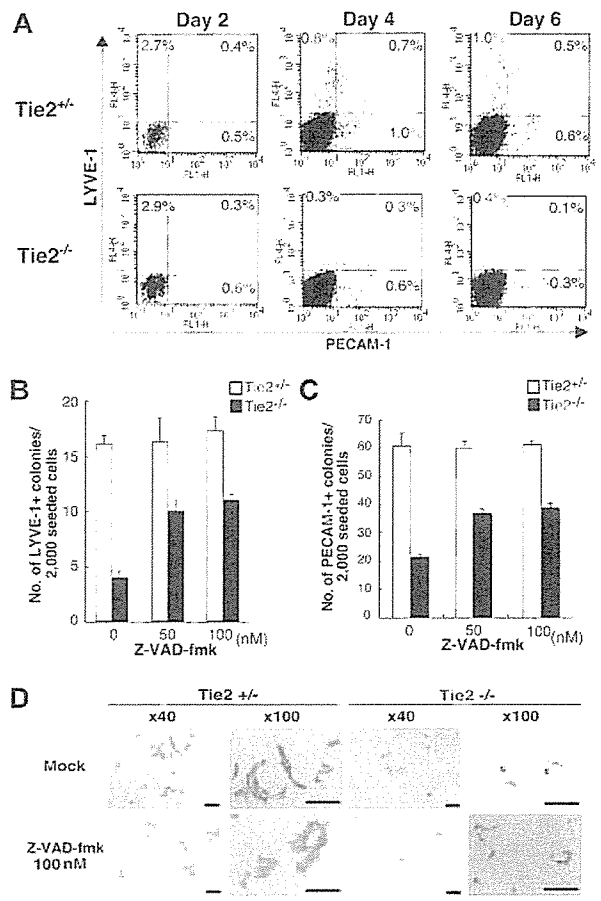

Figure 5. Tie2 signaling in blood vessels and lymphatic endothelial cells protected from apoptosis. (A) Expression of PECAM-1 and LYVE-1 in ES cell–derived cells was analyzed by flow cytometry at days 2, 4, and 6 of culture. The percentages of cells in each quadrant are indicated. (B) Addition of the caspase inhibitor Z-VAD-fmk (50 nM) to the culture media rescued the number of LYVE-1$^+$ colonies from *Tie2*$^{-/-}$ ES cells (■). (C) The number of PECAM-1$^+$ colonies from *Tie2*$^{-/-}$ ES cells (■) was also rescued in the presence of Z-VAD-fmk (50 nM). Results are expressed as mean ± SD. (D) In the presence of Z-VAD-fmk, the size of *Tie2*$^{-/-}$ lymphatic endothelial cells was unchanged, although the number of lymphatic colonies was partially rescued. Scale bars, 20 μm.

development of hematopoietic and endothelial lineages. Using an ES cell differentiation system, we have analyzed the development of hematopoietic cells as well as BECs and LECs from *Tie2*$^{-/-}$ ES cells. At day 8 of culture on OP9 cells, the normal formation of hematopoietic clusters from *Tie2*$^{-/-}$ cells suggests that Tie2 signaling does not contribute to development of hematopoietic cells from precursors. Furthermore, differentiation of myeloid cells from *Tie2*$^{-/-}$ hematopoietic clusters was normal. These results indicate that Tie2 is not essential for development of hematopoietic cells from ES cells. Recently, Puri and Bernstein[21] used combined mosaic analysis to demonstrate that Tie receptors are not required for differentiation and proliferation of definitive hematopoietic lineages in the embryo and fetus. Their findings are consistent with what we show in this study. Although our in vitro differentiation experiments suggest that Tie2 is not essential for hematopoiesis during development, Ang1/Tie2 signaling in hematopoietic cells has been reported to function to maintain hematopoietic stem cells in the bone marrow niche where Ang1 is expressed by osteoblasts.[18] Thus Tie2 function in hematopoiesis would seem to be specific for adult bone marrow.

Although much is known about normal and pathologic development of the vascular system,[35] the lack of specific markers has made it difficult to follow the development of the lymphatic system. In order to identify LECs, we recently generated a LEC-specific mAb against LYVE-1.[26] This mAb allowed us to detect LECs in mouse embryos at midgestation and purify these cells. ES cell–derived LYVE-1$^+$ cells express LEC-specific genes, such as *Prox1*, *Pdpn*, and *VEGFR3*, and exhibit DiI-Ac-LDL uptake. Furthermore, VEGF-C and VEGF-D, lymphatic growth factors, increased the number of LYVE-1–positive endothelial colonies from ES cells. These findings indicate that LYVE-1$^+$ cells isolated from these cultures have many characteristics of LECs. Lymphatic vasculature of the thoracic and abdominal viscera have been proposed to arise by endothelial spreading from lymph sacs.[6,36] This proposal is supported by the finding that budding of endothelial cells from the veins of Prox-1 mutant embryos is arrested.[9,10] To clarify the mechanisms of lymphangiogenesis in vitro, we analyzed the function of Tie2. In this study LECs were differentiated from ES cell–derived Tie2$^+$Flk1$^+$ cells, and approximately 1% of Tie2$^+$Flk1$^+$ cells formed lymphatic endothelial colonies on OP9 cells. Our in vitro differentiation assay allows us to clarify the mechanisms of LEC development from its precursor.

Thus far, Tie2 signaling has been reported to be required for proper development and function of the vascular system. Mice lacking Ang2 exhibit lymphatic vessel defects, strongly suggesting a role of Tie2 signaling in lymphangiogenesis.[37] In this study we have shown that LECs and BECs can be differentiated from Tie2$^+$Flk1$^+$ cells, and that 65% of LYVE-1$^+$ LECs express Tie2. To analyze the function of Tie2 in the development of lymphatic endothelial cells, we performed FACS analysis and immunocytochemistry during differentiation of *Tie2*$^{-/-}$ ES cells. FACS analysis revealed that *Tie2*$^{-/-}$ cells expressing LYVE-1 decreased over time as did PECAM-1$^+$ BECs. Treatment with a caspase inhibitor, which specifically inhibits apoptosis, partially rescued defective formation of lymphatic and blood vessel endothelial colonies from *Tie2*$^{-/-}$ cells, suggesting that both endothelial cells undergo apoptosis in the absence of Tie2 signaling. Although Tie2 signaling contributed to the survival of both LECs and BECs on OP9 cells, treatment with the caspase inhibitor did not affect the size of *Tie2*$^{-/-}$ colonies. Based on these findings, we propose that Tie2 cooperates with other signaling pathways involved in growth. Although we do not identify these pathways, OP9 cells are known to secrete several growth factors, including VEGF-C and VEGF-D.[38] FACS analysis also revealed that at day 2 of culture, the frequency of LYVE-1$^+$ and PECAM-1$^+$ cells derived from *Tie2*$^{-/-}$ cells was comparable with frequencies seen in *Tie2*$^{+/-}$ cells, suggesting that lymphatic and blood vessel endothelial precursors develop normally from *Tie2*$^{-/-}$ cells. A gene expression study clearly showed that expression levels of Prox-1 in lymphatic precursors (the Flk1$^+$ cell fraction) of *Tie2*$^{-/-}$ cells were comparable with those seen in *Tie2*$^{+/-}$ cells, suggesting that Tie2 deficiency does not affect Prox-1 expression. These findings suggest that Tie2 is not essential for development of lymphatic and blood vessel endothelial precursors, although both types of endothelial cells from *Tie2*$^{-/-}$ cells undergo apoptosis due to lack of Tie2 signaling.

Regarding vascular endothelial cells, in vivo study has shown that mice lacking Ang1 and Tie2 develop a fairly normal primary vasculature, but that this vasculature fails to undergo further normal remodeling.[28,39,40] We have demonstrated that lymphatic endothelial cells express Tie2 in both embryonic and adult settings, and that the activation of Tie2 signaling by Ang1 stimulates both in vivo lymphatic angiogenesis in mouse cornea and in vitro colony formation of lymphatic endothelial cells.[26] Data from both in vitro ES cell differentiation and in vivo embryonic development suggest that Ang/Tie2 signaling may contribute to regulation of lymphatic vessel formation in the development of lymphatic vessels.

In summary, our results derived from induction studies of ES cells have revealed that Tie2 is expressed in the precursors of mesodermal lineages, hematopoietic cells, and endothelial cells. We have also shown that Tie2 is not essential for development of hematopoietic cells, but that it plays an important role in antiapoptotic signaling in lymphatic and blood vessel development.

Acknowledgment

We thank Ms Ayami Ono for expert assistance in the FACS analysis.

References

1. Sabin F. Studies on the origin of blood vessels and red corpuscles as seen in the living blastoderm of the chick during the second day of incubation. Contribut Embryol. 1920;9:213-262.
2. Kubo H, Alitalo K. The bloody fate of endothelial stem cells. Genes Dev. 2003;17:322-329.
3. Haar JL, Ackerman GA. A phase and electron microscopic study of vasculogenesis and erythropoiesis in the yolk sac of the mouse. Anat Rec. 1971;170:199-223.
4. Hamaguchi I, Huang XL, Takakura N, et al In vitro hematopoietic and endothelial cell development from cells expressing TEK receptor in murine aorta-gonad-mesonephros region. Blood. 1999; 93:1549-1556.
5. Choi K, Kennedy M, Kazarov A, Papadimitriou JC, Keller G. A common precursor for hematopoietic and endothelial cells. Development. 1998; 125:725-732.
6. Sabin FR. On the origin of the lymphatic system from the veins, and the development of the lymph hearts and thoracic duct in the pig. Am J Anat. 1902;1:367-389.
7. Oliver G, Detmar M. The rediscovery of the lymphatic system: old and new insights into the development and biological function of the lymphatic vasculature. Genes Dev. 2002;16:773-783.
8. Jeltsch M, Kaipainen A, Joukov V, et al. Hyperplasia of lymphatic vessels in VEGF-C transgenic mice. Science. 1997;276:1423-1425.
9. Wigle JT, Oliver G. Prox1 function is required for the development of the murine lymphatic system. Cell. 1999;98:769-778.
10. Wigle JT, Harvey N, Detmar M, et al. An essential role for Prox1 in the induction of the lymphatic endothelial cell phenotype. EMBO J. 2002;21: 1505-1513.
11. Shalaby F, Rossant J, Yamaguchi TP, et al. Failure of blood-island formation and vasculogenesis in Flk-1-deficient mice. Nature. 1995;376:62-66.

12. Shalaby F, Ho J, Stanford WL, et al. A requirement for Flk1 in primitive and definitive hematopoiesis and vasculogenesis. Cell. 1997;89:981-990.
13. Millauer B, Wizigmann-Voos S, Schnurch H, et al. High affinity VEGF binding and developmental expression suggest Flk-1 as a major regulator of vasculogenesis and angiogenesis. Cell. 1993;72:835-846.
14. Dumont DJ, Fong GH, Puri MC, Gradwohl G, Alitalo K, Breitman ML. Vascularization of the mouse embryo: a study of flk-1, tek, tie, and vascular endothelial growth factor expression during development. Dev Dyn. 1995;203:80-92.
15. de Vries C, Escobedo JA, Ueno H, Houck K, Ferrara N, Williams LT. The fms-like tyrosine kinase, a receptor for vascular endothelial growth factor. Science. 1992;255:989-991.
16. Dumont DJ, Gradwohl GJ, Fong GH, Auerbach R, Breitman ML. The endothelial-specific receptor tyrosine kinase, tek, is a member of a new subfamily of receptors. Oncogene. 1993;8:1293-1301.
17. Iwama A, Hamaguchi I, Hashiyama M, Murayama Y, Yasunaga K, Suda T. Molecular cloning and characterization of mouse TIE and TEK receptor tyrosine kinase genes and their expression in hematopoietic stem cells. Biochem Biophys Res Commun. 1993;195:301-309.
18. Arai F, Hirao A, Ohmura M, et al. Tie2/angiopoietin-1 signaling regulates hematopoietic stem cell quiescence in the bone marrow niche. Cell. 2004;118:149-161.
19. Takakura N, Huang XL, Naruse T, et al. Critical role of the TIE2 endothelial cell receptor in the development of definitive hematopoiesis. Immunity. 1998;9:677-686.
20. Hsu HC, Ema H, Osawa M, Nakamura Y, Suda T, Nakauchi H. Hematopoietic stem cells express Tie-2 receptor in the murine fetal liver. Blood. 2000;96:3757-3762.
21. Puri MC, Bernstein A. Requirement for the TIE family of receptor tyrosine kinases in adult but not fetal hematopoiesis. Proc Natl Acad Sci U S A. 2003;100:12753-12758.
22. Koblizek TI, Weiss C, Yancopoulos GD, Deutsch U, Risau W. Angiopoietin-1 induces sprouting angiogenesis in vitro. Curr Biol. 1998;8:529-532.
23. Papapetropoulos A, Garcia-Cardena G, Dengler TJ, Maisonpierre PC, Yancopoulos GD, Sessa WC. Direct actions of angiopoietin-1 on human endothelium: evidence for network stabilization, cell survival, and interaction with other angiogenic growth factors. Lab Invest. 1999;79:213-223.
24. Kwak HJ, So JN, Lee SJ, Kim I, Koh GY. Angiopoietin-1 is an apoptosis survival factor for endothelial cells. FEBS Lett. 1999;448:249-253.
25. Jones N, Voskas D, Master Z, Sarao R, Jones J, Dumont DJ. Rescue of the early vascular defects in Tek/Tie2 null mice reveals an essential survival function. EMBO Rep. 2001;2:438-445.
26. Morisada T, Oike Y, Yamada Y, et al. Angiopoietin-1 promotes LYVE-1-positive lymphatic vessel formation. Blood. 2005;105:4649-4656.
27. Tammela T, Saaristo A, Lohela M, et al. Angiopoietin-1 promotes lymphatic sprouting and hyperplasia. Blood. 2005;105:4624-4648.
28. Dumont DJ, Gradwohl G, Fong GH, et al Dominant-negative and targeted null mutations in the endothelial receptor tyrosine kinase, tek, reveal a critical role in vasculogenesis of the embryo. Genes Dev. 1994;8:1897-1909.
29. Puri MC, Rossant J, Alitalo K, Bernstein A, Partanen J. The receptor tyrosine kinase TIE is required for integrity and survival of vascular endothelial cells. EMBO J. 1995;14:5884-5891.
30. Yagi T, Tokunaga T, Furuta Y, et al. A novel ES cell line, TT2, with high germline-differentiating potency. Anal Biochem. 1993;214:70-76.
31. Hooper M, Hardy K, Handyside A, Hunter S, Monk M. HPRT-deficient (Lesch-Nyhan) mouse embryos derived from germline colonization by cultured cells. Nature. 1987;326:292-295.
32. Nagy A, Rossant J, Nagy R, Abramow-Newerly W, Roder JC. Derivation of completely cell culture-derived mice from early-passage embryonic stem cells. Proc Natl Acad Sci U S A. 1993;90:8424-8428.
33. Takakura N, Yoshida H, Ogura Y, Kataoka H, Nishikawa S. PDGFR alpha expression during mouse embryogenesis: immunolocalization analyzed by whole-mount immunohistostaining using the monoclonal anti-mouse PDGFR alpha antibody APA5. J Histochem Cytochem. 1997;45:883-893.
34. Yano M, Iwama A, Nishio H, Suda J, Takada G, Suda T. Expression and function of murine receptor tyrosine kinases, TIE and TEK, in hematopoietic stem cells. Blood. 1997;89:4317-4326.
35. Gale NW, Yancopoulos GD. Growth factors acting via endothelial cell-specific receptor tyrosine kinases: VEGFs, angiopoietins, and ephrins in vascular development. Genes Dev. 1999;13:1055-1066.
36. Gray H. In Anatomy of the human body. In: Clemente CD, ed. The Lymphatic System. Philadelphia, PA: Lea and Febiger; 1985:866-932.
37. Gale NW, Thurston G, Hackett SF, et al. Angiopoietin-2 is required for postnatal angiogenesis and lymphatic patterning, and only the latter role is rescued by Angiopoietin-1. Dev Cell. 2002;3:411-423.
38. Matsumura K, Hirashima M, Ogawa M, et al. Modulation of VEGFR-2-mediated endothelial-cell activity by VEGF-C/VEGFR-3. Blood. 2003;101:1367-1374.
39. Suri C, Jones PF, Patan S, et al. Requisite role of angiopoietin-1, a ligand for the TIE2 receptor, during embryonic angiogenesis. Cell. 1996;87:1171-1180.
40. Sato TN, Tozawa Y, Deutsch U, et al. Distinct roles of the receptor tyrosine kinases Tie-1 and Tie-2 in blood vessel formation. Nature. 1995;376:70-74.